Supplementary Material Available: A table of anisotropic thermal parameters and listing of observed and calculated structure amplitudes (11 pages). Ordering information is given on any current masthead page.

References and Notes

(1) T. Peters and F. A. Blumenstock, *J. Biol. Chem.*, **242**, 1574 (1967).
(2) W. T. Shearer, R. A. Bradshaw, and F. R. N. Gurd, *J. Biol. Chem.*, **242**, 5451 (1967).
(3) R. A. Bradshaw, W. T. Shearer, and F. R. N. Gurd, *J. Biol. Chem.*, **243**, 3817 (1968).
(4) T. P. A. Kruck and B. Sarkar, *Inorg. Chem.*, **14**, 2383 (1975), and references therein.
(5) L. F. Wong, J. C. Cooper, and D. W. Margerum, *J. Am. Chem. Soc.*, **98**, 7268 (1976), and references therein.
(6) R. P. Agarwal and D. D. Perrin, *J. Chem. Soc., Dalton Trans.*, 53, (1977).
(7) N. Camerman, A. Camerman, and B. Sarkar, *Can. J. Chem.*, **54**, 1309 (1976).
(8) P. de Meester and D. J. Hodgson, *J. Am. Chem. Soc.*, **98**, 7086 (1976).
(9) R. B. Wilson, P. de Meester, and D. J. Hodgson, *Inorg. Chem.*, in press.
(10) (a) J. F. Blount, K. A. Frazer, H. C. Freeman, J. T. Szymanski, and C-H. Wang, *Acta Crystallogr.*, **22**, 396 (1967); (b) J. F. Blount, H. C. Freeman, R. V. Holland, and G. H. W. Milburn, *J. Biol. Chem.*, **245**, 5177 (1970).
(11) M. B. Hursthouse, S. A. A. Jeyaweara, G. H. W. Milburn, and A. Quick, *Chem. Commun.*, 207 (1971).
(12) P. W. R. Corfield, R. J. Doedens, and J. A. Ibers, *Inorg. Chem.*, **6**, 197 (1967).
(13) "International Tables for X-Ray Crystallography", Vol. IV, Kynoch Press, Birmingham, England, 1974.
(14) R. F. Stewart, E. R. Davidson, and W. T. Simpson, *J. Chem. Phys.*, **42**, 3175 (1965).
(15) D. T. Cromer and D. Liberman, *J. Chem. Phys.*, **53**, 1891 (1970).
(16) W. H. Zachariasen, *Acta Crystallogr., Sect. A*, **24**, 212 (1968).
(17) P. de Meester and D. J. Hodgson, *Acta Crystrallogr.*, in press.
(18) R. Osterberg, B. Sjoberg, and R. Soderquist, *Acta Chem. Scand.*, **26**, 4184 (1972).
(19) A. C. Andrews and E. W. Grundemeier, *J. Inorg. Nucl. Chem.*, **28**, 455 (1966).
(20) R. W. Hay in "Metal Ions in Biological Systems", Vol. 5, H. Sigel, Ed., Marcel Dekker, New York, N.Y., 1976, Chapter 3.
(21) W. H. Starnes, *J. Am. Chem. Soc.*, **86**, 5603 (1964).
(22) C. A. Grob and A. Weiss, *Helv. Chim. Acta*, **43**, 1340 (1960).
(23) J. Kazan and F. D. Greene, *J. Org. Chem.*, **28**, 2965 (1963).
(24) J. K. Kochi, *J. Am. Chem. Soc.*, **87**, 3609 (1965).
(25) J. D. Bacha and J. K. Kochi, *Tetrahedron*, **24**, 2215 (1968).
(26) S. P. Datta, A. K. Grzybowski, and S. S. Tate, *Nature (London)*, **207**, 1047 (1965).
(27) J. H. Fitzpatrick, Jr., and D. Gopgood, *Inorg. Chem.*, **13**, 568 (1974).

Contribution from the School of Chemical Sciences, University of Illinois, Urbana, Illinois 61801

Magnetic Exchange Interactions in Transition-Metal Dimers. 12. Structural and Magnetic Characterization of the Di-μ(1,3)-azido Complex $[Cu_2(Me_5dien)_2(N_3)_2](BPh_4)_2$ and Similar Di-μ(1,3)-azido Copper(II) Dimers. Unusual Zero-Field Splitting in the Electron Paramagnetic Resonance Spectra[1]

TIMOTHY R. FELTHOUSE and DAVID N. HENDRICKSON*[2]

Received June 16, 1977

The crystal and molecular structure of $[Cu_2(Me_5dien)_2(N_3)_2](BPh_4)_2$, where Me_5dien is 1,1,4,7,7-pentamethyldiethylenetriamine, has been determined using heavy-atom, least-squares, x-ray methods for 3140 reflections measured on a computer-automated four-circle diffractometer. The complex crystallizes as dark green prisms belonging to the space group $P2_1/n$ with two formula weights in a unit cell with a = 12.798 (2) Å, b = 19.538 (3) Å, c = 13.072 (2) Å, β = 93.64 (1)°, ρ_{obsd} = 1.215 g/cm^3, and ρ_{calcd} = 1.218 g/cm^3. The structure was refined to final discrepancy indices of R_F = 0.051 and R_{wF} = 0.058. The complex consists of discrete $[Cu_2(Me_5dien)_2(N_3)_2]^{2+}$ cations located about centers of inversion and BPh_4^- anions. The five-coordinate geometry about the copper(II) ion is intermediate between square pyramidal and trigonal bipyramidal. The two azide ions, which are parallel, are bridging in an end-to-end fashion between the two copper(II) ions. Each azide ion bonds at appreciably different distances, Cu–N = 1.985 (4) and 2.252 (5) Å, to the two copper(II) ions. The copper(II) ions are only 0.0504 (5) Å out of the azide plane and the Cu–Cu distance is 5.2276 (7) Å. Variable-temperature (4.2–270 K) magnetic susceptibility and EPR (X- and Q-band) data are reported for this Me_5dien and for five other analogous di-μ(1,3)-azido copper(II) dimers of the composition $[Cu_2(\text{"dien"})_2(N_3)_2](X)_2$, where "dien" is variously Et_5dien or dpt (dipropylenetriamine) and X^- is BPh_4^- or ClO_4^-. Antiferromagnetic exchange interactions are found for five of the six compounds with exchange parameters ranging from −3.1 cm^{-1} (Me_5dien, ClO_4^-) to −11.1 cm^{-1} (Et_5dien, ClO_4^-). These results are discussed in terms of the local copper(II) ion geometry which is enforced by the "dien" ligand and various other structural and electronic factors. The X-band EPR spectra for powdered *undoped* samples of the BPh_4^- salts exhibit copper(II) hyperfine structure as well as zero-filled splittings which are appropriate for the triplet state of such a dimer. The magnitude of zero-field splitting observed for these complexes greatly exceeds that calculated for purely dipolar interactions and, as such, the presence of pseudodipolar interactions is suggested. Pseudodipolar zero-field interactions, which result from spin–orbit admixture of excited states and depend on the exchange interactions in the excited states, were unexpected and indicate exchange interactions in the excited states that are greater than those observed for the ground state.

Introduction

In a previous paper in this series,[3] the magnitude of the magnetic exchange interaction between two copper(II) ions was found to be dependent upon the oribtal ground state composition of the copper(II) ions. A series of complexes of the type $[Cu_2(\text{"dien"})_2(C_2O_4)](BPh_4)_2$ was studied in which the relatively inflexible oxalate dianion ($C_2O_4^{2-}$) bridges the two copper(II) ions in a bis-bidentate fashion and in which "dien" is dien (diethylenetriamine), dpt (dipropylenetriamine), Me_5dien (1,1,4,7,7-pentamethyldiethylenetriamine), or Et_5dien (1,1,4,7,7-pentaethyldiethylenetriamine). Consequently, the local environment about the copper(II) ion could be changed from square pyramidal with dien to trigonal bipyramidal with Et_5dien.

When two azide ions are substituted for the oxalate dianion in the above complexes, two types of bridging modes could

0020-1669/78/1317-0444$01.00/0

result (L = dien, dpt, Me_5dien, Et_5dien):

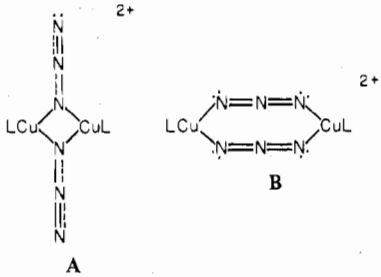

A B

Recent review articles[4-6] have suggested that type B bridging is favored whenever nonbonded repulsions of the nonbridging ligands become significant. Among structurally characterized di-μ-azide-bridged complexes of copper, type A bridging has been found in polymeric $Cu(bpy)(N_3)_2$[7] (bpy = 2,2′-bipyridine), while type B bridging has been reported in the dimeric copper(I) complex $Cu_2(PPh_3)_4(N_3)_2$.[8] Both kinds of bridging occur in polymeric $Cu(N_3)_2$.[9]

In our previous studies of copper(II) complexes involving the azide ion, the dimeric formulations of $[Cu_2(tren)_2(N_3)_2](BPh_4)_2$[10] (tren = 2,2′,2″-triaminotriethylamine) and $[Cu_2(dien)_2(N_3)_2](BPh_4)_2$[10,11] were confirmed by IR and EPR spectra although the mode of azide bridging could not be characterized definitively. No magnetic exchange interaction could be detected in the magnetic susceptibility data to 4.2 K for either complex, but the Q-band EPR spectrum of the dien complex showed a hyperfine pattern appropriate for a copper(II) dimer in the solid state. It was decided to prepare additional analogous "dien" dimers to see if di-μ-azide-bridged copper(II) complexes could be prepared that do show the presence of a magnetic exchange in the susceptibility. The EPR properties of these compounds proved to be very interesting and, as such, the structure of $[Cu_2(Me_5dien)_2(N_3)_2](BPh_4)_2$ was solved. The results of the structural work are reported in this paper. Additionally, in this paper we report the variable-temperature (4.2–270 K) magnetic susceptibility and EPR (6–300 K) data for the series $[Cu_2(\text{"dien"})_2(N_3)_2](X)_2$, where "dien" is dpt, Me_5dien, or Et_5dien and X^- is BPh_4^- or ClO_4^-. A preliminary account of the structural and magnetic properties of $[Cu_2(Me_5dien)_2(N_3)_2](BPh_4)_2$ has been reported previously.[12]

Experimental Section

Compound Preparation. Dipropylenetriamine (Aldrich), 1,1,4,-7,7-pentamethyldiethylenetriamine (Ames Laboratories, Inc.), and 1,1,4,7,7-pentaethyldiethylenetriamine (Ames Laboratories, Inc.) were used as received. Elemental analyses were performed by the Microanalytical Laboratory of the School of Chemical Sciences, University of Illinois. The analytical data are compiled in Table I.[13]

Samples of **$[Cu_2(\text{"dien"})_2(N_3)_2](BPh_4)_2$**, where "dien" is dpt, Me_5dien, or Et_5dien, were prepared by the following general procedure. To an aqueous solution of ca. 0.005 mol of $Cu(ClO_4)_2\cdot 6H_2O$ was added ca. 0.005 mol of "dien" followed by an aqueous solution of ca. 1.6 g (0.025 mol, fivefold excess) of NaN_3. Addition of the "dien" ligand first prevents formation of large amounts of *potentially explosive* $Cu(N_3)_2$. The mixture was filtered and an aqueous solution of ca. 0.5 g of $NaPBh_4$ was added, yielding a green solid which was washed with water and then diethyl ether and dried in a vacuum desiccator. Alternatively, to a solution of $[Cu_2(\text{"dien"})_2(N_3)_2](ClO_4)_2$ in ca. 7:1 methanol–water was added a filtered methanol solution of $NaBPh_4$. After a few seconds, the dark green microcrystalline product formed.

Preparation of the $[Cu_2(\text{"dien"})_2(N_3)_2](ClO_4)_2$ complexes was accomplished by using 1:1 water–ethanol solutions and stoichiometric amounts of $Cu(ClO_4)_2\cdot 6H_2O$, "dien", and NaN_3. Evaporation of the solvents yielded sky blue plates for **$[Cu_2(dpt)_2(N_3)_2](ClO_4)_2$** and greenish black needles for **$[Cu_2(Me_5dien)_2(N_3)_2](ClO_4)_2$** and **$[Cu_2(Et_5dien)_2(N_3)_2](ClO_4)_2$**.

Samples of **$Cu(\text{"dien"})(N_3)_2$**, where "dien" is Me_5dien or Et_5dien, were prepared by a procedure given by Gray, et al.[14] To a 150-mL aqueous solution of ca. 0.01 mol of $CuSO_4\cdot 5H_2O$ was added ca. 0.01 mol of "dien". After mixing with 50 mL of water containing ca. 3 g of NaN_3, the mixture was extracted with three 200-mL portions of CH_2Cl_2. These portions were dried with $MgSO_4$ and evaporated completely to give the crude product. Dissolution of this solid in a 2:1 methanol–1-butanol mixture followed by slow evaporation led to a dark green crystalline product. The solids were dried extensively on a vacuum line and in a vacuum desiccator over P_4O_{10}. The dark green crystals, when powdered, give a brownish orange solid for **$Cu(Et_5dien)(N_3)_2$** and a yellowish green solid for **$Cu(Me_5dien)(N_3)_2$**.

The zinc complex **$[Zn_2(Me_5dien)_2(N_3)_2](BPh_4)_2$** was prepared for use in EPR doping experiments. The Et_5dien analogue could not be prepared apparently due to the formation of $Zn(OH)_2$. Acidification of these mixtures led to the protonation of Et_5dien.

Physical Measurements. Variable-temperature (4.2–270 K) magnetic susceptibility and EPR measurements were performed as described in a recent paper.[3] The susceptibility data were least-squares fit to the Bleaney–Bowers equation[15] ($\mathcal{H} = -2J\hat{S}_1\cdot\hat{S}_2$).

Crystal Measurements. The diffraction data for **$[Cu_2(Me_5dien)_2(N_3)_2](BPh_4)_2$** were collected by Molecular Structure Corp., while the structure solution and refinement were performed at the University of Illinois.

A dark green prismatic crystal of **$[Cu_2(Me_5dien)_2(N_3)_2](BPh_4)_2$** with dimensions of 0.21 × 0.23 × 0.25 mm was mounted on a glass fiber. Preliminary examination of the crystal and data collection were performed on a Syntex $P\bar{1}$ four-circle automatic diffractometer. On the basis of 15 computer-centered reflections, the crystal was found to be monoclinic with the space group $P2_1/n$ based on the systematic absences, $0k0$, $k = 2n + 1$, and $h0l$, $h + l = 2n + 1$. The cell constants were determined from a least-squares refinement of the setting angles for the 15 reflections and are given in Table II along with the details of the data collection. Three standard reflections were monitored periodically as a check on the crystal and electronic stability and no significant change in the counting statistics was found. Lorentz and

Table II. Experimental Data for the X-Ray Diffraction Study of $[Cu_2(Me_5dien)_2(N_3)_2](BPh_4)_2$

Crystal Parameters	
$a = 12.798$ (2) Å	Space group: $P2_1/n$
$b = 19.538$ (3) Å	$Z = 4$ (2 dimers)
$c = 13.072$ (2) Å	Mol wt 1196.21
$\beta = 93.64$ (1)°	$\rho_{calcd} = 1.218$ g cm^{-3}
$V = 3262.1$ (9) Å^3	$\rho_{obsd} = 1.215$ g cm^{-3} (flotation in toluene–bromotoluene)

Measurement of Intensity Data

Radiation: Mo Kα, λ 0.710 73 Å
Monochromator: graphite crystal
Takeoff angle: 3°
Counter aperature: 2.0 mm
X-ray beam collimator diameter: 1.5 mm
Crystal-detector distance: 190 mm
Crystal orientation: random
Width at half-height from ω scans: 0.2°
Reflections measured: $+h,+k,\pm l$
Maximum 2θ: 45°
Scan type: θ–2θ scan technique
Scan speed: variable, 4–24° min^{-1}
Scan range: from 2θ (Mo Kα_1) − 0.8° to 2θ (Mo Kα_2) + 0.8°
Background measurement: stationary crystal, stationary counter, $R = 2.0$[a]
Reflections collected: 4266 unique reflections, 3140 observed above 3σ cutoff
Temperature: 23 ± 1 °C

Treatment of Intensity Data

Calculation of intensity I: $I = S(C - RB)$;[a,b] $\sigma(I) = [S^2(C + R^2B) + (pI)^2]^{1/2}$[c]
Conversion to $|F_o|$ and $\sigma(F_o)$: $|F_o| = (I/Lp)^{1/2}$;[d] $\sigma(F_o) = \sigma(I)/2|F_o|(Lp)$
Absorption coeff. 7.29 cm^{-1}
$F(000)$: 1388

[a] R = ratio of scan time to background counting time. [b] S = scan rate, C = total integrated peak count, B = total background count. [c] $p = 0.07$ (downweights intense reflections). [d] Lp = Lorentz-polarization factor.

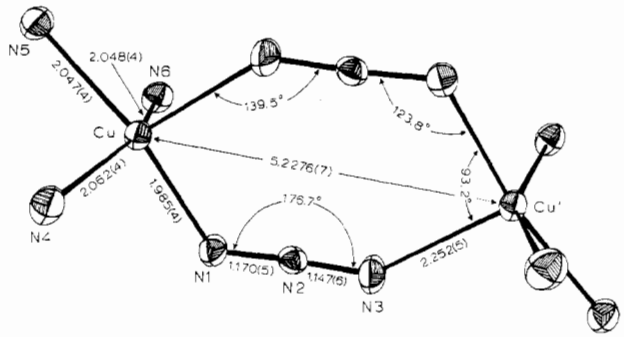

Figure 1. ORTEP plotting of the inner coordination sphere and di-μ-azido bridging geometry of $[Cu_2(Me_5dien)_2(N_3)_2]^{2+}$ showing principal bond distances and angles. The dimer is located about a center of inversion.

polarization corrections were applied to the data. Extinction and absorption corrections were not necessary.

Structure Solution and Refinement. A three-dimensional Patterson map was calculated using the 3140 observed reflections and the heavy-atom vectors gave the copper atom position at $x = 0.076$, $y = 0.083$, and $z = 0.141$. This corresponded to an intradimer copper atom separation of 5.19 Å. The copper atom position with an isotropic thermal parameter was refined twice using the computer program ORFLS (Busing and Levy). This atom position was used to generate a Fourier map. Spherical-atom scattering factors were used in this and subsequent calculations as given by Hansen, et al.[16a] for hydrogen, boron, nitrogen, and copper, while carbon atom scattering factors were from Cromer and Mann.[16b] The real and imaginary components of anomalous dispersion were included for the copper atom.[16c]

From the Fourier map, it was possible to locate all 41 nonhydrogen atoms in the asymmetric unit. Two cycles of full-matrix least-squares refinement of the overall scale factor and the positional parameters were followed by two more cycles in which the isotropic thermal parameters were also varied. The function minimized was $\sum w||F_o| - |F_c||^2$, where $w = 1/(\sigma(F_o))^2$ and $\sigma(F_o)$ is defined in Table II. At this point, the refinement had reached convergence with $R_F = \sum(|F_o| - |F_c|)/\sum|F_o| = 0.104$ and $R_{wF} = (\sum w|F_o - F_c|^2/\sum wF_o^2)^{1/2} = 0.125$. With anisotropic thermal parameters for all 41 nonhydrogen atoms, the refinement proceeded in two parts. First, the dimeric cation parameters were varied followed by variation of the BPh_4^- anion parameters. After two such cycles of refinement of the cation and anion parameters, the hydrogen atom positions were generated using the program HYGEN (F. K. Ross). The carbon–hydrogen distances were taken as 0.95 Å and it was assumed that the ethylene and methyl carbon atoms of the Me_5dien ligand were sp^3 hybridized while the phenyl carbon atoms of the BPh_4^- anion possessed sp^2 hybridization. The hydrogen atoms were assigned the thermal parameters for the carbon atom to which they were attached in the refined model using isotropic thermal parameters. Two more cycles of refinement including anisotropic thermal parameters on both the cation and anion nonhydrogen atoms led to convergence with $R_F = 0.051$ and $R_{wF} = 0.058$. Another cycle of refinement of the cation parameters resulted in parameter shifts of less than half the estimated standard deviations. The expected error in a measurement of unit weight (erf) is defined by $[\sum w(|F_o| - |F_c|)^2/(NO - NV)]^{1/2}$, where the number of reflections (NO) was 3140 and the number of refined parameters (NV) was 145 and 226 for the cation and anion, respectively. The final erf value for the cation was 1.05, while for the anion the erf was 1.06. A final difference-Fourier map showed no peaks or depressions greater than 0.40 e/Å^3 in any region. The final values of $|F_o|$ and $|F_c|$ for the 4266-reflection data set appear as supplementary material.

Results and Discussion

Molecular Structure of $[Cu_2(Me_5dien)_2(N_3)_2](BPh_4)_2$. The single-crystal structure of $[Cu_2(Me_5dien)_2(N_3)_2](BPh_4)_2$ was solved. The final positional and anisotropic thermal parameters are presented in Table III and Table IV,[13] respectively, while bond distances and angles are given in Table V.

The structure consists of discrete dimeric $[Cu_2(Me_5dien)_2(N_3)_2]^{2+}$ cations and BPh_4^- anions. The dimeric cation is located about a crystallographic center of inversion. In Figure 1 is shown a perspective view of the inner coordination about each copper(II) ion and the two bridging azide ions. As can be seen, each azide ion bridges in an end-to-end fashion and this leads to a relatively large Cu–Cu distance of 5.2276 (7) Å within the dimeric cation. The di-μ(1,3)-azido bridging in this complex forms a nearly planar $Cu_2(N_3)_2$ ring with the Cu(II) ions 0.0504 (5) Å out of the azide plane (see Table VI[13]). Each azide ion bridges in an asymmetric fashion such that the Cu–N bond lengths are 1.985 (4) and 2.252 (5) Å; however, the azide ions are nearly linear with N(1)–N(2)–N(3) = 176.7 (5)°. Previously reported structures for transition-metal dimeric complexes incorporating end-to-end bridging azide ions include $Cu_2(PPh_3)_4(N_3)_2$,[8] $[Ni_2(macro)_2(N_3)_3]I$[17] (macro is 1,4,8,11-tetramethyl-1,4,8,11-tetraazacyclotetradecane), and $[Ni_2(tren)_2(N_3)_2](BPh_4)_2$.[18] Among all of these complexes, only in $[Cu_2(Me_5dien)_2(N_3)_2]^{2+}$ do the N(1)–N(2) and N(2)–N(3) bond lengths differ by a significant amount. In this case the bond lengths are 1.170 (5) and 1.147 (6) Å, respectively, while in the other three complexes these bond lengths are equal (ca. 1.17 Å). In several nondimeric copper(II) azide complexes involving coordination to a single end of the azide ion,[7,9,19,20] however, small differences in the two azide bond lengths have been noted which are apparently due to the covalency in the Cu(II)–N bond. In $Cu(Et_4dien)(Br)(N_3)$[21] (Et_4dien is 1,1,7,7-tetraethyldiethylenetriamine) the bond lengths are equal.

The coordination geometries about the five-coordinate Cu(II) ions in $[Cu_2(Me_5dien)_2(N_3)_2]^{2+}$ are best described as intermediate between a square pyramid and a trigonal bipyramid. A comparison of the Cu(II) ion stereochemistry with known[22] pentacoordinate geometries substantiates this comment. The stereoscopic plotting of the dimeric cation $[Cu_2(Me_5dien)_2(N_3)_2]^{2+}$ in Figure 2 best illustrates the coordination geometry about the Cu(II) ion and presents the labeling scheme used for the nonhydrogen atoms of the dimeric cation.[23] When the Cu(II) ion coordination geometry is viewed as a square pyramid, the three Me_5dien nitrogen atoms N(4), N(5), and N(6) and the azide atom N(1) comprise the square plane and the azide nitrogen atom N(3)′ from the other azide bonds is placed into the apical position at 2.252 (5) Å from the Cu(II) ion. However, a least-squares plane calculation for this plane (Table VI[13]) shows that the four nitrogen atoms

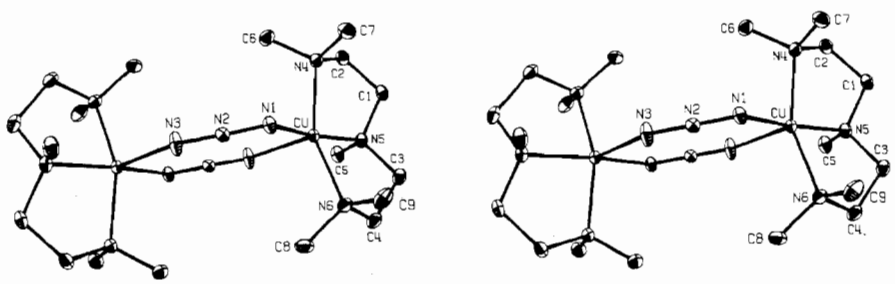

Figure 2. Stereoscopic ORTEP plotting of $[Cu_2(Me_5dien)_2(N_3)_2]^{2+}$ with the atom numbering scheme as indicated; the hydrogen atoms are not shown.

Table III. Final Positional Parameters for All Atoms in $[Cu_2(Me_5dien)_2(N_3)_2](BPh_4)_2$,[a] Including Isotropic Thermal Parameters for Hydrogen Atoms[b]

Atom	x	y	z	Atom	x	y	z
Cu	0.06746 (4)	0.08628 (3)	0.14206 (4)	C(16)	0.1943 (4)	0.2793 (3)	0.4813 (4)
N(1)	0.0746 (3)	−0.0152 (2)	0.1462 (3)	C(21)	−0.0432 (3)	0.1948 (2)	0.5903 (3)
N(2)	0.0404 (3)	−0.0506 (2)	0.0801 (3)	C(22)	−0.0699 (4)	0.1388 (2)	0.6498 (4)
N(3)	0.0086 (4)	−0.0880 (2)	0.0181 (3)	C(23)	−0.1608 (4)	0.1011 (2)	0.6306 (4)
N(4)	0.2249 (3)	0.0930 (2)	0.1181 (3)	C(24)	−0.2302 (4)	0.1182 (3)	0.5507 (4)
N(5)	0.0740 (3)	0.1902 (2)	0.1610 (3)	C(25)	−0.2079 (4)	0.1722 (3)	0.4896 (3)
N(6)	−0.0575 (3)	0.0890 (2)	0.2325 (3)	C(26)	−0.1155 (3)	0.2096 (2)	0.5092 (3)
C(1)	0.1867 (4)	0.2069 (2)	0.1807 (4)	C(31)	0.0379 (3)	0.2924 (2)	0.7188 (3)
C(2)	0.2491 (4)	0.1660 (3)	0.1093 (4)	C(32)	0.0915 (4)	0.3535 (3)	0.7350 (4)
C(3)	0.0112 (5)	0.2052 (3)	0.2491 (4)	C(33)	0.0743 (4)	0.3973 (3)	0.8157 (5)
C(4)	−0.0871 (4)	0.1623 (3)	0.2401 (4)	C(34)	−0.0006 (5)	0.3819 (3)	0.8834 (4)
C(5)	0.0315 (5)	0.2288 (3)	0.0703 (4)	C(35)	−0.0553 (4)	0.3223 (3)	0.8703 (4)
C(6)	0.2551 (4)	0.0555 (3)	0.0270 (4)	C(36)	−0.0362 (4)	0.2787 (2)	0.7900 (4)
C(7)	0.2834 (4)	0.0634 (3)	0.2088 (4)	C(41)	0.1568 (4)	0.1871 (2)	0.6584 (4)
C(8)	−0.1486 (4)	0.0490 (3)	0.1929 (5)	C(42)	0.1793 (4)	0.1317 (3)	0.5970 (4)
C(9)	−0.0229 (5)	0.0613 (3)	0.3342 (4)	C(43)	0.2642 (5)	0.0883 (3)	0.6195 (5)
C(11)	0.0995 (3)	0.2878 (2)	0.5279 (3)	C(44)	0.3282 (4)	0.0982 (3)	0.7063 (5)
C(12)	0.0392 (4)	0.3425 (3)	0.4900 (4)	C(45)	0.3070 (4)	0.1506 (3)	0.7702 (5)
C(13)	0.0682 (5)	0.3849 (3)	0.4113 (5)	C(46)	0.2230 (4)	0.1941 (3)	0.7467 (4)
C(14)	0.1613 (6)	0.3724 (3)	0.3672 (4)	B	0.0625 (4)	0.2405 (3)	0.6235 (4)
C(15)	0.2247 (5)	0.3209 (3)	0.4025 (5)				

Atom	x	y	z	B, Å^2	Atom	x	y	z	B, Å^2
H(12)	−0.0287	0.3505	0.5202	4.51	H(53) (C(2))	0.3225	0.1738	0.1243	4.65
H(13)	0.0246	0.4236	0.3873	5.77	H(54)	0.2325	0.1811	0.0397	4.65
H(14)	0.1806	0.3999	0.3083	5.84	H(55) (C(3))	−0.0066	0.2531	0.2521	5.21
H(15)	0.2919	0.3135	0.3728	6.06	H(56)	0.0492	0.1939	0.3128	5.21
H(16)	0.2411	0.2424	0.5079	4.89	H(57) (C(4))	−0.1282	0.1768	0.1783	5.16
H(22)	−0.0223	0.1259	0.7081	4.15	H(58)	−0.1290	0.1702	0.2965	5.16
H(23)	−0.1759	0.0622	0.6737	4.39	H(59) (C(5))	−0.0392	0.2181	0.0547	5.33
H(24)	−0.2947	0.0925	0.5369	4.30	H(60)	0.0407	0.2762	0.0807	5.33
H(25)	−0.2575	0.1838	0.4346	3.83	H(61)	0.0707	0.2159	0.0112	5.33
H(26)	−0.1015	0.2472	0.4639	3.49	H(62) (C(6))	0.2392	0.0073	0.0334	5.83
H(32)	0.1451	0.3661	0.6885	4.47	H(63)	0.2176	0.0721	−0.0332	5.83
H(33)	0.1152	0.4386	0.8227	5.07	H(64)	0.3283	0.0596	0.0188	5.83
H(34)	−0.0148	0.4140	0.9381	5.23	H(65) (C(7))	0.2692	0.0156	0.2152	5.41
H(35)	−0.1082	0.3119	0.9188	5.02	H(66)	0.3583	0.0681	0.2023	5.41
H(36)	−0.0751	0.2356	0.7835	4.37	H(67)	0.2666	0.0861	0.2697	5.41
H(42)	0.1336	0.1229	0.5353	5.82	H(68) (C(8))	−0.1323	0.0011	0.1857	6.84
H(43)	0.2786	0.0494	0.5746	6.24	H(69)	−0.2061	0.0528	0.2351	6.84
H(44)	0.3881	0.0684	0.7230	5.73	H(70)	−0.1729	0.0647	0.1243	6.84
H(45)	0.3529	0.1578	0.8302	5.36	H(71) (C(9))	−0.0009	0.0139	0.3309	6.49
H(46)	0.2090	0.2304	0.7955	4.03	H(72)	0.0395	0.0862	0.3624	6.49
H(51) (C(1))	0.2091	0.1959	0.2493	5.02	H(73)	−0.0741	0.0649	0.3827	6.49
H(52)	0.1981	0.2548	0.1698	5.02					

[a] Standard deviations of the least significant figures are in parentheses and are given in this fashion in succeeding tables. The hydrogen atom positions were computed geometrically based upon the positions of the atoms to which they are bound. Tetraphenylborate carbon and hydrogen atoms are numbered as in ref 23. The other hydrogen atoms are bonded to the carbon atoms given in parentheses or the atoms immediately above them. [b] The hydrogen atoms were given the isotropic temperature factor obtained from the last isotropic least-squares refinement for the atom to which they are bound.

deviate from a plane by ca. 0.15 Å and that the Cu(II) ion is displaced 0.3159 (5) Å from the plane toward atom N(3)′. Alternatively, a trigonal-bipyramidal description of the Cu(II) ion environment places atoms N(3)′, N(4), and N(6) in the trigonal plane with the axial positions taken by the secondary nitrogen atom N(5) of Me_5dien and the azide atom N(1). The Cu(II) ion deviates only 0.0821 (5) Å from the trigonal plane. The trigonal axis shows some distortion from linearity with N(1)–Cu–N(5) = 170.4 (2)°; the trigonal angles also depart significantly from the idealized 120° with values of 103.1 (2), 103.2 (2), and 153.1 (2)°.

The effect of complete alkylation of the dien (diethylenetriamine) ligand to give Me_5dien appears to be a distortion away from a trans positioning of the terminal nitrogen atoms (as was noted in a previous paper in this series[3]) to cis coordination positions in which the central (secondary) nitrogen atom occupies an axial site. In addition to $[Cu_2(Me_5dien)_2(N_3)_2](BPh_4)_2$, three other structures have been reported which involve the Me_5dien ligand: $Co(Me_5dien)Cl_2$,[24] $Cu(Me_5dien)(NCBH_3)_2$,[25] and, very recently, $[Cu_2(Me_5dien)_2(CA)](BPh_4)_2$,[1] where CA^{2-} is the dianion of chloranilic acid. For these Me_5dien complexes, the degree of distortion from the trans coordination of the terminal nitrogen atoms can be gauged by the N(4)–M–N(6) angles (see Figures 1 and 2) which are found to be 153.1 (2), 151.8 (2), 151.9 (1), and 135° for $[Cu_2(Me_5dien)_2(N_3)_2](BPh_4)_2$, $[Cu_2(Me_5dien)_2(CA)](BPh_4)_2$, $Cu(Me_5dien)(NCBH_3)_2$, and $Co(Me_5dien)Cl_2$, respectively. The effect is even more pronounced when bulkier ethyl groups are substituted on the dien ligand. The N(4)–M–N(6) angle reduces further toward the 120° value expected for a trigonal bipyramid as in the case of $[Cu_2(Et_5dien)_2(C_2O_4)](BPh_4)_2$ [131.4 (2)°],[3] $Cu(Et_4dien)(Br)(N_3)$ [128.8 (2)°],[21] and $Co(Et_4dien)Cl_2$ [120.4 (4)°].[26] In short, the complexes with Me_5dien have metal ion coordination geometries that are intermediate between SP and TBP. In $[Cu_2(Me_5dien)_2(N_3)_2]^{2+}$, the Cu–N bond lengths of the Me_5dien ligand are nearly equal with values of 2.062 (4), 2.047 (4), and 2.048 (4) Å.

A stereoscopic view of the unit cell can be seen in Figure 3 and this clearly shows the role of the BPh_4^- anions in isolating

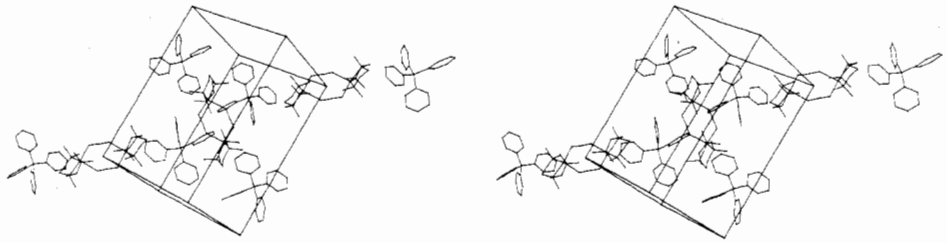

Figure 3. Stereoscopic packing diagram of $[Cu_2(Me_5dien)_2(N_3)_2](BPh_4)_2$; the hydrogen atoms have been omitted.

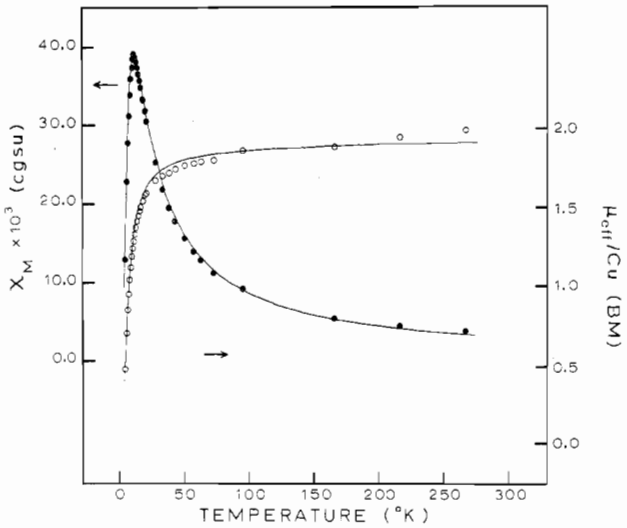

Figure 4. Experimental molar paramagnetic susceptibility (●) per dimer and effective magnetic moment (○) per Cu(II) ion vs. temperature for $[Cu_2(Me_5dien)_2(N_3)_2](BPh_4)_2$. The solid lines represent the least-squares fit to the Bleaney–Bowers equation.

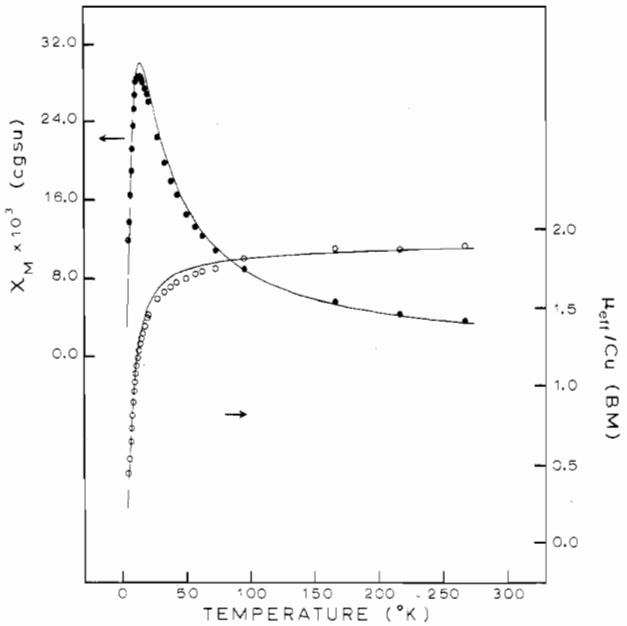

Figure 5. Experimental molar paramagnetic susceptibility (●) per dimer and effective magnetic moment (○) per Cu(II) ion vs. temperature for $[Cu_2(Et_5dien)_2(N_3)](BPh_4)_2$ using the Bleaney–Bowers equation to generate the least-squares fit solid lines.

the Cu(II) dimers. As a result, the closest *inter*dimer Cu–Cu distance is 10.9218 (7) Å. *Inter*dimer magnetic exchange interactions should be minimal. As will be described, the large interdimer Cu–Cu distances lead to well-resolved EPR spectra for the *pure undoped* compound.

All distances and angles in the tetraphenylborate anion appear normal. The least-squares planes for the phenyl groups and the corresponding dihedral angles are given in Table VI.[13] All of the phenyl rings are essentially planar; the average C–C distance is 1.384 (8) Å and the average B–C distance is 1.649 (7) Å. Our previous work[23,27] with BPh_4^- shows consistently that the carbon atom attached to the boron atom has the smallest phenyl ring angle (average 114.5 (4)°), while the ortho carbon atoms show the largest angles (average 123.1 (5)°).

Magnetic Susceptibility. Variable-temperature magnetic susceptibility data for complexes of the form $[Cu_2(\text{"dien"})_2(N_3)_2](BPh_4)_2$, where "dien" is variously dpt, Me_5dien, or Et_5dien, are collected in Tables VII–IX.[13] A representative plotting of magnetic susceptibility and moment vs. temperature is illustrated in Figure 4 for $[Cu_2(Me_5dien)_2(N_3)_2](BPh_4)_2$. The susceptibility increases with decreasing temperature until a maximum is reached at ca. 11 K, after which the susceptibility decreases. The magnetic moment varies from 1.99 μ_B at 267 K to 0.46 μ_B at 4.2 K. Least-squares fitting of the susceptibility data to the Bleaney–Bowers equation[15] gives $J = -6.5$ cm^{-1} with $g = 2.200$. The solid lines in Figure 4 represent this fit.

Antiferromagnetic interactions have also been found for $[Cu_2(Et_5dien)_2(N_3)_2](BPh_4)_2$ and $[Cu_2(dpt)_2(N_3)_2](BPh_4)_2$. Figure 5 illustrates the data for the Et_5dien complex for which the magnetic moment decreases from 1.90 μ_B at 267 K to 0.44 μ_B at 4.2 K with a maximum in the susceptibility curve at ca. 13 K. The least-squares fit parameters for the Et_5dien compound are $J = -8.3$ cm^{-1} and $g = 2.174$. In the case of the dpt complex a somewhat weaker interaction is present; see Figure 6. The maximum in the magnetic susceptibility data occurs at ca. 7.4 K and least-squares fitting of the susceptibility data yields $J = -4.5$ cm^{-1} and $g = 2.180$.

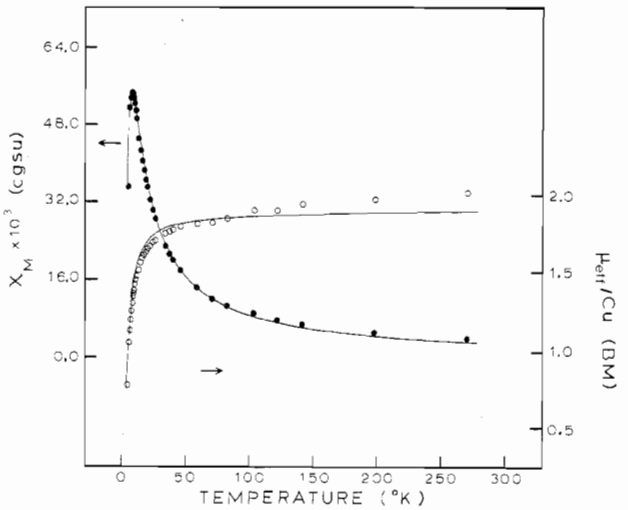

Figure 6. Experimental molar paramagnetic susceptibility (●) per dimer and effective magnetic moment (○) per Cu(II) ion vs. temperature for $[Cu_2(dpt)_2(N_3)_2](BPh_4)_2$. The solid lines were generated from the least-squares fit to the Bleaney–Bowers equation.

Three additional complexes of the form $[Cu_2(\text{"dien"})_2(N_3)_2](ClO_4)_2$ have been prepared in order to evaluate the

Table V. Principal Interatomic Distances (Å) and Angles (deg) for $[Cu_2(Me_5dien)_2(N_3)_2](BPh_4)_2$

Distances within $[Cu_2(Me_5dien)_2(N_3)_2]^{2+}$			
Cu-Cu′	5.2276 (7)	N(4)-C(7)	1.479 (7)
Cu-N(1)	1.985 (4)	N(5)-C(1)	1.485 (7)
Cu-N(3)′	2.252 (5)	N(5)-C(3)	1.476 (7)
Cu-N(4)	2.062 (4)	N(5)-C(5)	1.479 (7)
Cu-N(5)	2.047 (4)	N(6)-C(4)	1.487 (7)
Cu-N(6)	2.048 (4)	N(6)-C(8)	1.470 (7)
N(1)-N(2)	1.170 (5)	N(6)-C(9)	1.478 (7)
N(2)-N(3)	1.147 (6)	C(1)-C(2)	1.497 (7)
N(4)-C(2)	1.466 (6)	C(3)-C(4)	1.509 (8)
N(4)-C(6)	1.471 (7)		
Angles within $[Cu_2(Me_5dien)_2(N_3)_2]^{2+}$			
N(1)-Cu-N(3)′	93.2 (2)	C(6)-N(4)-C(7)	107.9 (4)
N(1)-Cu-N(4)	91.4 (2)	Cu-N(5)-C(1)	105.7 (3)
N(1)-Cu-N(5)	170.4 (2)	Cu-N(5)-C(3)	105.7 (3)
N(1)-Cu-N(6)	92.7 (2)	Cu-N(5)-C(5)	113.5 (3)
N(3)′-Cu-N(4)	103.1 (2)	C(1)-N(5)-C(3)	113.1 (4)
N(3)′-Cu-N(5)	96.3 (2)	C(1)-N(5)-C(5)	109.3 (4)
N(3)′-Cu-N(6)	103.2 (2)	C(3)-N(5)-C(5)	109.5 (4)
N(4)-Cu-N(5)	85.6 (1)	Cu-N(6)-C(4)	106.0 (3)
N(4)-Cu-N(6)	153.1 (2)	Cu-N(6)-C(8)	114.5 (3)
N(5)-Cu-N(6)	86.1 (2)	Cu-N(6)-C(9)	108.0 (3)
Cu-N(1)-N(2)	123.8 (3)	C(4)-N(6)-C(8)	109.6 (4)
N(1)-N(2)-N(3)	176.7 (5)	C(4)-N(6)-C(9)	110.9 (4)
Cu-N(3)′-N(2)′	139.5 (4)	C(8)-N(6)-C(9)	107.9 (4)
Cu-N(4)-C(2)	106.7 (3)	N(5)-C(1)-C(2)	109.0 (4)
Cu-N(4)-C(6)	113.6 (3)	N(4)-C(2)-C(1)	110.2 (4)
Cu-N(4)-C(7)	107.7 (3)	N(5)-C(3)-C(4)	108.7 (4)
C(2)-N(4)-C(6)	110.7 (4)	N(6)-C(4)-C(3)	109.0 (4)
C(2)-N(4)-C(7)	110.2 (4)		
Distances in the Tetraphenylborate Anion			
C(11)-C(12)	1.390 (7)	C(31)-C(32)	1.388 (7)
C(12)-C(13)	1.390 (8)	C(32)-C(33)	1.386 (8)
C(13)-C(14)	1.379 (10)	C(33)-C(34)	1.378 (8)
C(14)-C(15)	1.356 (9)	C(34)-C(35)	1.363 (9)
C(15)-C(16)	1.386 (8)	C(35)-C(36)	1.385 (7)
C(16)-C(11)	1.402 (7)	C(36)-C(31)	1.397 (7)
C(21)-C(22)	1.397 (6)	C(41)-C(42)	1.388 (7)
C(22)-C(23)	1.386 (7)	C(42)-C(43)	1.395 (8)
C(23)-C(24)	1.369 (7)	C(43)-C(44)	1.370 (9)
C(24)-C(25)	1.365 (7)	C(44)-C(45)	1.360 (9)
C(25)-C(26)	1.401 (7)	C(45)-C(46)	1.389 (8)
C(26)-C(21)	1.392 (6)	C(46)-C(41)	1.395 (7)
B-C(11)	1.648 (7)	B-C(31)	1.652 (7)
B-C(21)	1.656 (7)	B-C(41)	1.638 (7)
Angles in the Tetraphenylborate Anion			
C(12)-C(11)-C(16)	114.4 (4)	C(32)-C(31)-C(36)	114.4 (4)
C(13)-C(12)-C(11)	123.7 (5)	C(33)-C(32)-C(31)	123.1 (5)
C(14)-C(13)-C(12)	118.8 (6)	C(34)-C(33)-C(32)	120.3 (5)
C(15)-C(14)-C(13)	120.2 (6)	C(35)-C(34)-C(33)	118.5 (5)
C(16)-C(15)-C(14)	119.9 (6)	C(36)-C(35)-C(34)	120.5 (5)
C(11)-C(16)-C(15)	123.0 (5)	C(31)-C(36)-C(35)	123.2 (5)
C(22)-C(21)-C(26)	114.4 (4)	C(42)-C(41)-C(46)	114.7 (4)
C(23)-C(22)-C(21)	123.2 (4)	C(43)-C(42)-C(41)	122.6 (5)
C(24)-C(23)-C(22)	120.3 (5)	C(44)-C(43)-C(42)	120.4 (6)
C(25)-C(24)-C(23)	119.1 (5)	C(45)-C(44)-C(43)	118.8 (6)
C(26)-C(25)-C(24)	120.1 (4)	C(46)-C(45)-C(44)	120.5 (5)
C(21)-C(26)-C(25)	122.9 (4)	C(41)-C(46)-C(45)	122.9 (5)
B-C(11)-C(12)	121.4 (4)	C(11)-B-C(21)	111.9 (4)
B-C(11)-C(16)	124.2 (4)	C(11)-B-C(31)	107.7 (4)
B-C(21)-C(22)	120.1 (4)	C(11)-B-C(41)	109.0 (4)
B-C(21)-C(26)	125.4 (4)	C(21)-B-C(31)	109.7 (4)
B-C(31)-C(32)	121.9 (4)	C(21)-B-C(41)	107.8 (4)
B-C(31)-C(36)	123.7 (4)	C(31)-B-C(41)	110.7 (4)
B-C(41)-C(42)	120.8 (4)		
B-C(41)-C(46)	124.5 (4)		

effect of the counterion on the magnetic properties of the Cu(II) dimers. The susceptibility data (Table X[13]) for $[Cu_2(Me_5dien)_2(N_3)_2](ClO_4)_2$ show a maximum at ca. 6 K and fit to give $J = -3.1$ cm^{-1} and $g = 2.080$. This is a weaker interaction than is present in the corresponding BPh_4^- salt. In contrast, $[Cu_2(Et_5dien)_2(N_3)_2](ClO_4)_2$ with $J = -11.1$ cm^{-1} and a maximum in the magnetic susceptibility at ca. 19 K

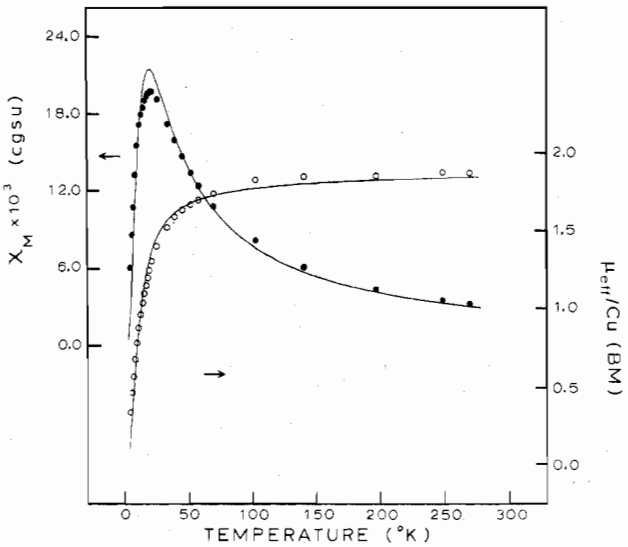

Figure 7. Experimental molar paramagnetic susceptibility (●) per dimer and effective magnetic moment (○) per Cu(II) ion vs. temperature for $[Cu_2(Et_5dien)_2(N_3)_2](ClO_4)_2$ using the Bleaney–Bowers equation to generate the least-squares fit solid lines.

Table XIII. Summary of Magnetic Susceptibility Fitting Data for Azide-Bridged Copper(II) Dimers

Compd	J, cm^{-1}	$\bar{g}$[a]	SE[b]
$[Cu_2(Me_5dien)_2(N_3)_2](BPh_4)_2$	−6.5	2.200	0.0408
$[Cu_2(Et_5dien)_2(N_3)_2](BPh_4)_2$	−8.3	2.174	0.0660
$[Cu_2(dpt)_2(N_3)_2](BPh_4)_2$	−4.5	2.180	0.0469
$[Cu_2(dien)_2(N_3)_2](BPh_4)_2$[c]	$\lesssim 0.5$[d]	2.112	
$[Cu_2(Me_5dien)_2(N_3)_2](ClO_4)_2$	−3.1	2.080	0.0329
$[Cu_2(Et_5dien)_2(N_3)_2](ClO_4)_2$	−11.1	2.130	0.0857
$[Cu_2(dpt)_2(N_3)_2](ClO_4)_2$	$\lesssim 0.5$[d]	2.110	
$[Cu_2(tren)_2(N_3)_2](BPh_4)_2$[e]	$\lesssim 0.5$[d]	2.13	
$[Cu_2(tet\text{-}b)_2(N_3)](ClO_4)_3$[f]	−13.7	2.01	

[a] Average g values obtained from magnetic susceptibility fitting except if $|J| \lesssim 0.5$ cm^{-1}; then EPR values are given. [b] Standard error (SE) given by $SE = \{\sum_{i=1}^{NP}[\mu_{eff}(obsd)_i - \mu_{eff}(calcd)_i]^2/(NP-k)\}^{1/2}$ where k is the number of variable parameters used to fit the NP data points (see A. P. Ginsberg, R. L. Martin, R. W. Brookes, and R. C. Sherwood, *Inorg. Chem.*, **11**, 2884 (1972)). [c] Reference 11. [d] In these cases there are no signs of an exchange interaction in the susceptibility to 4.2 K and so $|J| \lesssim 0.5$ cm^{-1}. [e] References 10 and 11. [f] Reference 28.

(data in Table XI;[13] see Figure 7) shows a somewhat stronger interaction than the corresponding BPh_4^- compound. And finally, in the case of $[Cu_2(dpt)_2(N_3)_2](ClO_4)_2$ (data in Table XII[13]), no interaction could be detected in the susceptibility data taken down to 4.2 K, and this means that $|J| \lesssim 0.5$ cm^{-1}.

The results of fitting the susceptibility data for all of the above azide complexes as well as some results for other azide-bridged Cu(II) dimers are summarized in Table XIII. An examination of the magnitude of exchange parameters in Table XIII reveals a trend toward a somewhat greater interaction as the triamine ligand in $[Cu_2(\text{"dien"})_2(N_3)_2]X_2$ changes the local Cu(II) ion geometry from predominantly square pyramidal with dien and dpt to greater trigonal-bipyramidal character with Me_5dien and Et_5dien. A similar correlation was observed[3] for the analogous μ-oxalato complexes where the exchange parameter varies from −37.4 cm^{-1} for $[Cu_2(Et_5dien)_2(C_2O_4)](BPh_4)_2$ to $|J| \lesssim 0.5$ cm^{-1} for $[Cu_2(dien)_2(C_2O_4)](ClO_4)_2$. In the μ-oxalato series, the Et_5dien complex has been shown to have TBP Cu(II) coordination geometry, whereas the geometry is known to be SP in the dien–oxalate compound. Besides the change in local Cu(II) ion coordination geometry, other factors which can influence the magnitude of exchange interaction in these types of complexes are the displacement of the Cu(II) ion out of

either the SP or TBP plane and the semicoordination of the counterion (notably ClO_4^-). In comparison to an oxalate bridge, a bridge between two Cu(II) ions that consists of two azide ions is more flexible and variable in structure. This greater variability makes it more difficult to present a definitive analysis of the change in exchange interaction in a series of di-μ(1,3)-azido-bridged complexes.

With two azide ions bridging in an end-to-end fashion to complete an eight-atom $Cu_2(N_3)_2$ ring, the relative orientation of each azide ion may be altered when different backside triamine (i.e., "dien") ligands are employed. In such a $Cu_2(N_3)_2$ dimer, attention can be drawn to two planes, each formed by one Cu(II) ion and the two nearest azide nitrogen atoms. It is possible to key on the dihedral angle between these two planes in analyzing the magnitude of magnetic exchange that is found. Such an approach was used to understand the magnetic exchange in two structurally characterized nickel(II) dimers[18] in which both mono-μ(1,3)-azido and di-μ(1,3)-azido bridging geometries were encountered. In the mono-μ-(1,3)-azido complex $[Ni_2(macro)_2(N_3)_3]I$ the exchange parameter was found to be -12.3 cm^{-1} while in the di-μ(1,3)-azido compound $[Ni_2(tren)_2(N_3)_2](BPh_4)_2$ a larger antiferromagnetic exchange interaction is present with $J = -35.1$ cm^{-1}. The nearly threefold increase in the exchange parameter was attributed to a larger admixture of $2p_x$ and $2p_y$ azide nitrogen bonding orbitals in the dibridged complex. This was substantiated with MO calculations[18] on $H_2N_3^+$ with different dihedral angles. The MO calculations showed that a dihedral angle of 38.4° (appropriate for $[Ni_2(tren)_2(N_3)_2](BPh_4)_2$) gave rise to a greater number of bridge bonding interactions than are present for $H_2N_3^+$ with a 0° dihedral angle, which is what is found for $[Ni_2(macro)_2(N_3)_3]I$.

A comparison of the metal–bridge bonding geometries of $Ni_2(N_3)_2$ in $[Ni_2(tren)_2(N_3)_2](BPh_4)_2$ and $Cu_2(N_3)_2$ in $[Cu_2(Me_5dien)_2(N_3)_2](BPh_4)_2$ provides a plausible explanation for the weaker antiferromagnetic interaction present in the copper compound ($J = -6.5$ cm^{-1}) compared to that found in the nickel compound ($J = -35.1$ cm^{-1}). Both dimers have essentially the same metal–metal distance [5.2276 (7) Å for Cu(II) and 5.220 (2) Å for Ni(II)]. There is a greater disparity in metal–nitrogen (azide) bond distances for the Cu(II) dimer: 1.985 (4) and 2.252 (5) Å for Cu(II) vs. 2.069 (8) and 2.195 (7) Å for Ni(II). The Cu(II) dimer has a dihedral angle between the Cu–N(1)–N(2) and Cu–N(2)–N(3) planes of only 5.0° compared to the 38.4° value for the Ni(II) dimer. Thus, it is probably the relatively long Cu–N distance of 2.252 (5) Å and the small dihedral angle that lead to the weaker interaction for the Cu(II) dimer. Single-crystal EPR work is needed to ascertain the details of the electronic ground state of the Cu(II) dimer.

Four other compounds have been reported which involve bridging azide ions. Previous work in these laboratories produced $[Cu_2(dien)_2(N_3)_2](BPh_4)_2$[10,11] and $[Cu_2(tren)_2(N_3)_2](BPh_4)_2$.[10] Magnetic susceptibilities down to 4.2 K were determined for both compounds and neither compound showed a magnetic exchange interaction. However, the dien compound did show copper hyperfine structure in the Q-band EPR spectrum that is characteristic of a dimer and, as such, the exchange parameter for this compound is $0.02 \text{ cm}^{-1} \lesssim |J| \lesssim 0.5 \text{ cm}^{-1}$. An analysis of the zero-field splitting observed in the EPR spectra of the dien compound led us to conclude that the azide ions were involved in outer-sphere (i.e., hydrogen bonding) bridging. In view of the structure of $[Cu_2(Me_5dien)_2(N_3)_2](BPh_4)_2$, it seems probable that the azide bridging in $[Cu_2(dien)_2(N_3)_2](BPh_4)_2$ is also of a direct inner-sphere type. The tren compound does not show any signs of an exchange interaction in the EPR spectrum.

A mono-μ-azido complex has been reported[28] having the composition $[Cu_2(tet\text{-}b)_2(N_3)](ClO_4)_3$, where tet-b is *rac*-5,5,7,12,12,14-hexamethyl-1,4,8,11-tetraazacyclotetradecane. The compound is presumably structured similarly to the μ-chloro copper(II) dimer $[Cu_2(tet\text{-}b)_2(Cl)](ClO_4)_3$, the structure of which has been reported.[29] In this mono-μ-azido complex, then, the azide ion apparently bridges between the equatorial positions of two TBP Cu(II) complexes. The exchange parameter[28] of -13.7 cm^{-1} exceeds any of the parameters of the di-μ(1,3)-azido Cu(II) dimers reported in this work. Finally, the azide ion has been found to be involved in both type A and type B bridging modes in polymeric $Cu(N_3)_2$.[9] The magnetic susceptibility data[30] show a Néel temperature of 259 K. The large antiferromagnetic interaction in $Cu(N_3)_2$ probably largely results from the type A azide bridging.

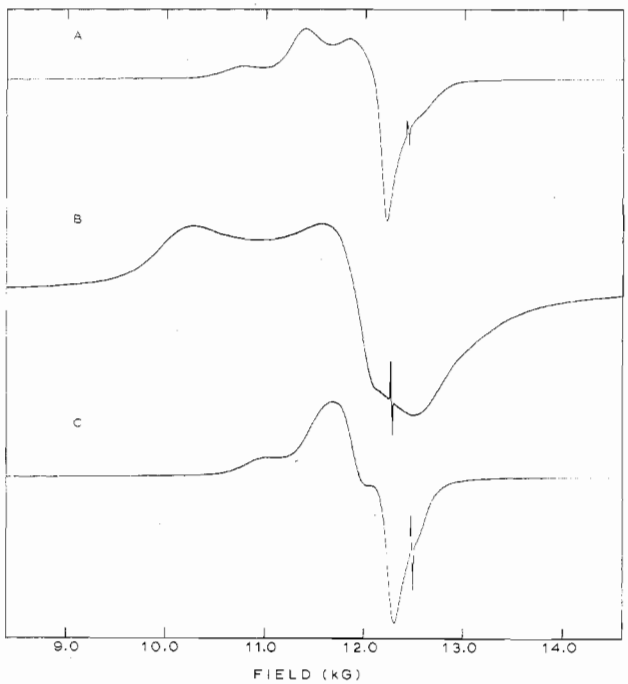

Figure 8. Q-Band (~35 GHz) EPR spectra of powdered samples of $[Cu_2(dpt)_2(N_3)_2](BPh_4)_2$ (A), $[Cu_2(Me_5dien)_2(N_3)_2](BPh_4)_2$ (B), and $[Cu_2(Et_5dien)_2(N_3)_2](BPh_4)_2$ (C) recorded at ~110 K. DPPH ($g = 2.0036$) is used as a frequency calibrant. Variations in the frequency cause the DPPH signal to occur at different field positions.

Electron Paramagnetic Resonance. X- and Q-band EPR spectra have been recorded for powdered *undoped* samples of all six of the copper–azide compounds in this study. Our previous work[1,3,10,11,31] has shown that the tetraphenylborate counterion offers distinct advantages in obtaining EPR observables from resolved spectra for undoped samples of Cu(II) dimers. These observables include singlet–triplet transitions, $\Delta M_s = 2$ transitions, and copper hyperfine structure on both the $\Delta M_s = 1$ and $\Delta M_s = 2$ signals. The tetraphenylborate anion provides a reasonably magnetically dilute environment for the copper dimer, thereby reducing *inter*dimer magnetic exchange interactions and *inter*dimer dipolar interactions. The tetraphenylborate salts of di-μ(1,3)-azido copper dimers in this study provide interesting examples of *undoped* dimeric Cu(II) dimers with rich EPR spectra.

The Q-band EPR spectra of $[Cu_2(Me_5dien)_2(N_3)_2](BPh_4)_2$, $[Cu_2(dpt)_2(N_3)_2](BPh_4)_2$, and $[Cu(Et_5dien)_2(N_3)_2](BPh_4)_2$ are shown in Figure 8. The spectra were recorded at ca. 110 K; however, no significant differences were observed from those recorded at room temperature. Perhaps the most notable feature in Figure 8 is the broadness of the spectrum of $[Cu_2(Me_5dien)_2(N_3)_2](BPh_4)_2$ in tracing B. The absorption for this compound extends over ca. 5000 G. This spectrum looks like an "axial" spectrum with the apparent "parallel"

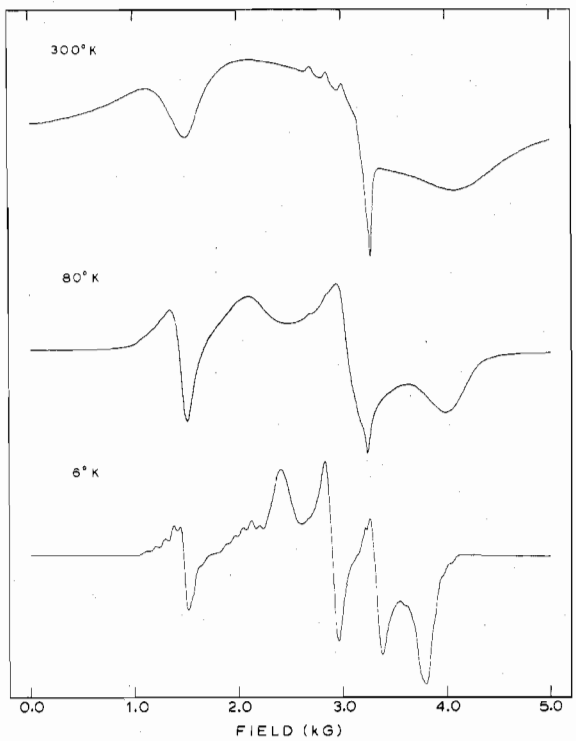

Figure 9. Temperature dependence of all visible features in the X-band EPR spectrum of a powdered sample of $[Cu_2(Me_5dien)_2(N_3)_2](BPh_4)_2$. The spectra were recorded at the following frequencies: 300 K, 9.0891 GHz; 80 K, 9.0902 GHz; 6 K, 9.1427 GHz.

and "perpendicular" g values occurring at 2.393 (10 270 G) and 2.067 (11 888 G), respectively A $\Delta M_s = 2$ transition can be seen at lower fields with ca. 0.05 times the intensity of the $\Delta M_s = 1$ transition; the $\Delta M_s = 2$ transition shows a "parallel" region at $g \approx 4.414$ (5620 G) and a "perpendicular" region at $g \approx 4.120$ (6020 G). The Q-band EPR spectrum of $[Cu_2(dpt)_2(N_3)_2](BPh_4)_2$ in tracing A of Figure 8 is narrower than that of the Me_5dien complex and it has "apparent" signals at g values of 2.306 (10 800 G), 2.185 (11 398 G), and 2.062 (12 077 G). Of similar appearance is the Q-band spectrum of the Et_5dien compound (tracing C) with "apparent" g values of 2.265 (11 038 G), 2.141 (11 678 G), and 2.032 (12 307 G). The dpt and Et_5dien complexes show $\Delta M_s = 2$ transitions of much weaker intensity than is observed for the Me_5dien complex. The unusual line widths and g values in these three Q-band spectra were puzzling until the X-band spectra were examined.

The temperature dependence (6–300 K) of all spectral features in the X-band EPR spectrum of $[Cu_2(Me_5dien)_2(N_3)_2](BPh_4)_2$ is shown in Figure 9. At 300 K, the spectrum consists of an extremely broad $\Delta M_s = 1$ region encompassing a field of several thousand gauss with a sharp feature at 3143 G. Three "bumps" at 2697, 2853, and 3005 G are also seen. These three bumps and some part of the sharp feature are undoubtedly due to a Cu(II) monomeric impurity. Several analytically pure samples of $[Cu_2(Me_5dien)_2(N_3)_2](BPh_4)_2$, including many that were recrystallized, were examined and it was found that these monomeric impurity features in the 300 K spectrum do vary from one sample to another (the low-temperature spectra did not vary). The susceptibility curve for this compound (Figure 4) does not show much of an indication of a monomeric impurity, but very little impurity is needed to affect the EPR spectrum. The $\Delta M_s = 2$ transition at 1395 G appears on the same scale as the broad $\Delta M_s = 1$ absorption in the 300 K spectrum.[32] Upon cooling the sample from 300 to 80 K, the signal intensity increases dramatically. With the modulation amplitude (25 G) and microwave power (20 mW) held constant, the 300 K spectrum was recorded with a relative receiver gain of 250 while at 80 K the gain was only 25. The 80 K spectrum shows somewhat improved resolution compared to the 300 K spectrum and also shows a loss in relative intensity of the impurity signal. However, cooling the sample to 6 K gives a spectrum with markedly improved resolution (the impurity signal is now not very visible).

The 6 K spectrum for $[Cu_2(Me_5dien)_2(N_3)_2](BPh_4)_2$ has the characteristic appearance of a triplet-state spectrum. Some difficulty was encountered in obtaining a spectrum which did not show saturation effects at this low temperature. The 6 K spectrum in Figure 9 was recorded with a relative receiver gain of 40 and a microwave power of only 0.5 mW, which approached the limits of the instrument's frequency-lock stability. A study of the appearance of the spectrum as a function of microwave power showed that this spectrum is free of distortions due to saturation. The various signals in the 6 K spectrum are assignable. The half-field ($\Delta M_s = 2$) transition, which at 80 K is beginning to show copper hyperfine structure, at 6 K appears as a seven-line hyperfine pattern at 1476 G with an average hyperfine spacing of 87 G. The $\Delta M_s = 1$ signals begin at a field setting just slightly higher than the highest field $\Delta M_s = 2$ transition. The $\Delta M_s = 1$ region shows three pairs of zero-field split transitions[33] which are indicative (as expected) of the rhombic (i.e., nonaxial) nature of the Cu(II) coordination geometry in $[Cu_2(Me_5dien)_2(N_3)_2]^{2+}$. In the region of 1897–2207 G, five copper hyperfine lines can be readily seen with an average spacing of 78 G, which is half of the value expected for a copper monomer.[34] The other two lines of this seven-line pattern are obscured by a $\Delta M_s = 1$ transition at 2410 G. There should be another seven-line pattern resulting from zero-field splitting and this second seven-line $\Delta M_s = 1$ pattern would be expected at a much higher field position. Examination of the spectrum shows two weak apparent copper hyperfine lines at 4050 and 3980 G which could be the two highest field components of the other seven-line $\Delta M_s = 1$ pattern. The seventh line in this pattern can be assigned to a small feature at 3600 G. This gives an average spacing of 76 G for this seven-line pattern in good agreement with the spacing from the other $\Delta M_s = 1$ pattern. The separation (i.e., effective zero-field splitting) between corresponding components in these two seven-line $\Delta M_s = 1$ patterns is 1703 G (0.159 cm^{-1}), which gives an associated g value of 2.194. The four remaining features can be assigned to two pairs of zero-field split signals in only one way to give g values that are reasonable. The second pair of zero-field split features occurs at 2410 and 3815 G. This 1405 G (0.131 cm^{-1}) splitting is centered about a g value of 2.099. This second pair of signals overlaps significantly with the pair that shows the hyperfine structure. The last two signals which both appear as derivatives can be assigned as the third pair. Without a simulation, it is difficult to assign the field position of either of these two signals. If the signal positions are taken where the derivatives cross the baseline, this gives resonance fields of 2903 and 3307 G and the effective zero-field splitting is 404 G (0.038 cm^{-1}) with a g value of 2.104. These values have a considerable uncertainty associated with them. These assignments of zero-field split signals should only be taken as tentative and are reported primarily to relate the order of magnitude of the splittings to the reader in the absence of more definitive single-crystal EPR data. It is clear that several of the "**g** tensor" components show appreciable zero-field splitting. The inequality of average copper hyperfine splittings between the $\Delta M_s = 1$ signals and the seven-line $\Delta M_s = 2$ pattern suggests that there is a noncoincidence of the **g** and **A** tensors of the dimer.[35,36]

The temperature dependence of the X-band EPR signal for $[Cu_2(Et_5dien)_2(N_3)_2](BPh_4)_2$ is illustrated in Figure 10.

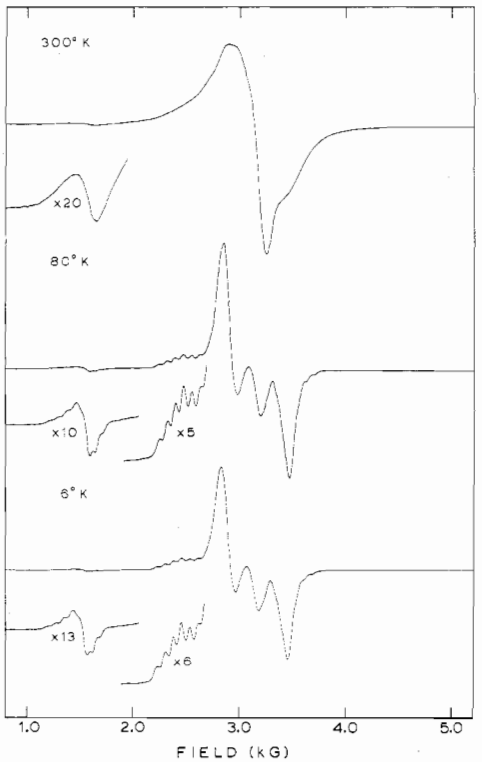

Figure 10. X-Band EPR spectra of all visible features of a powdered sample of $[Cu_2(Et_5dien)_2(N_3)_2](BPh_4)_2$ recorded at various temperatures with frequencies of 9.0900 GHz (300 K), 9.0910 GHz (80 K), and 9.1425 GHz (6 K).

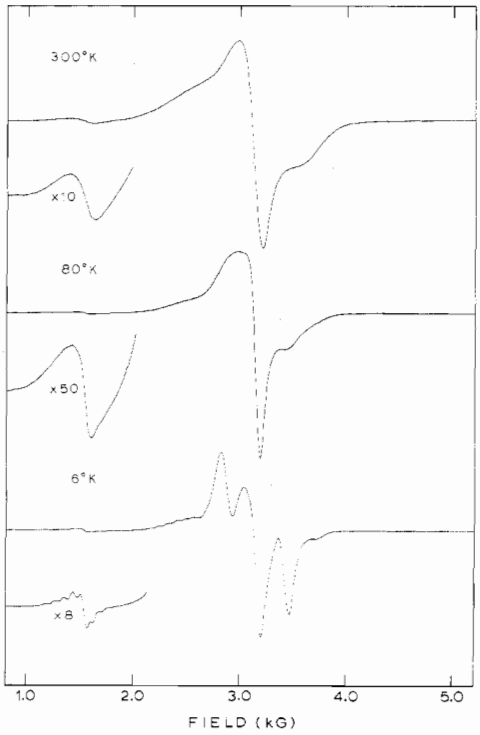

Figure 11. Temperature dependence of all visible features in the X-band and EPR spectrum of a powdered sample of $[Cu_2(dpt)_2(N_3)_2](BPh_4)_2$ recorded at the following frequencies: 9.0907 GHz (300 K), 9.0918 GHz (80 K), and 9.1472 GHz (6 K).

Again there is an improved resolution at the lower temperatures. At 300 K, the spectrum consists of a single asymmetric derivative at $g = 2.082$ with a "shoulder" on the high-field side at 3430 G ($g = 1.894$). A relatively weak $\Delta M_s = 2$ transition can be observed at 1580 G. Cooling the sample to 80 K results in the resolution of many spectral features associated with the triplet-state character of the dimer. In this case, unlike the Me_5dien case, additional cooling of the sample to 6 K does *not* result in much change in the spectrum. Furthermore, no effect of power saturation was noticed with microwave powers from 0.5 to 20 mW. The low-temperature spectrum of the Et_5dien compound is basically similar to that for the Me_5dien compound; however, the $\Delta M_s = 1$ region of the Et_5dien spectrum does not encompass as large a range of magnetic field. The $\Delta M_s = 2$ transition is also weaker for the Et_5dien compound. This feature is located at 1525 G and in this case nine copper hyperfine lines can be detected with an average spacing of 83 G. More than seven copper hyperfine lines on the $\Delta M_s = 2$ signal would only be observed when there is an appreciable rhombic component to the zero-field splitting. The lowest field $\Delta M_s = 1$ signal occurs at 2455 G with a seven-line copper hyperfine pattern (see insets) superimposed on it. Six of the seven lines are visible with an average spacing of 77 G. Two hyperfine components of the corresponding high-field seven-line pattern appear at 3610 and 3680 G. Assuming a 77-G average spacing between these lines places the high-field component of this zero-field split signal at 3456 G. This gives a 1001 G (0.094 cm^{-1}) effective zero-field splitting for $g = 2.210$. The second and third pairs of zero-field split absorptions have considerable overlap but can be assigned effective zero-field splittings of 630 G (0.059 cm^{-1}) and 263 G (0.025 cm^{-1}) for g values of 2.079 and 2.141, respectively.

The X-band EPR spectrum of $[Cu_2(dpt)_2(N_3)_2](BPh_4)_2$ as a function of temperature is shown in Figure 11. The 300 K spectrum is similar to that for the Et_5dien compound; however, in this case, cooling the sample to 80 K does not improve the resolution of the spectrum. At 6 K, the dpt spectrum resolves into three pairs of somewhat overlapping zero-field split absorptions in the $\Delta M_s = 1$ region. The spectrum was recorded at 0.5 mW microwave power since settings higher than this caused severe distortions in the line shapes due to saturation. A half-field transition is seen at 1528 G with nine copper hyperfine lines having an average spacing of 86 G (see inset below 6 K spectrum). The lowest field $\Delta M_s = 1$ signal (2410 G) again shows six copper hyperfine lines with an average separation of 80 G. Only one hyperfine component of the high-field seven-line counterpart can be located at 3710 G. If an 80-G separation is assumed to be present for this seven-line pattern, this places the center of the pattern at 3470 G. Thus, an effective zero-field splitting of 1060 G (0.099 cm^{-1}) is observed for this component with $g = 2.223$. The second and third pairs show effective zero-field splittings with g values of 2.082 and 2.093, respectively.

In summary, the X-band EPR spectra of $[Cu_2(Me_5dien)_2(N_3)_2](BPh_4)_2$, $[Cu_2(Et_5dien)_2(N_3)_2](BPh_4)_2$, and $[Cu_2(dpt)_2(N_3)_2](BPh_4)_2$ exhibit the interesting characteristics of unusual temperature dependencies in line widths and relatively large zero-field splittings.

In an attempt to account for the large zero-field splittings observed in the $\Delta M_s = 1$ region of the X-band spectrum of $[Cu_2(Me_5dien)_2(N_3)_2](BPh_4)_2$ at 6 K, various computer simulations were performed using a program written by Gibbons[37] which is based on the direct eigenfield method of Belford and co-workers.[38] The simulations involve numerical integration of a derivative spectrum over a large number of molecular orientations. A Hamiltonian operator incorporating Zeeman interactions, isotropic exchange, and *dipolar* zero-field splitting terms, but, due to prohibitive costs, excluding hyperfine interactions, was used. Data from the EPR spectra of copper(II) monomers possibly mimicking the local copper(II) geometry in $[Cu_2(Me_5dien)_2(N_3)_2](BPh_4)_2$ were used to help obtain reasonable estimates of possible g values for the dimer. For instance, a powdered sample of $Cu(Me_5dien)(N_3)_2$

gave a Q-band EPR spectrum indicative of a distorted TBP copper(II) geometry with g values of 2.185, 2.143, and 2.039. The Q-band spectrum of $Cu(Et_5dien)(N_3)_2$ was found to signal even less distortion from idealized TBP geometry with g values of 2.191, 2.164, and 2.012. On the other hand, an "axial" SP geometry was indicated by the spectrum of a sample containing 1% Cu^{2+} doped into $[Zn_2(Me_5dien)_2(N_3)_2](BPh_4)_2$ with $g_{\parallel}$ = 2.220 and $g_{\perp}$ = 2.054. This doped sample spectrum also shows four copper hyperfine lines on the $g_{\perp}$ signal with an average spacing of 158 G. It is recalled that the Me_5dien dimer exhibits copper hyperfine lines on two $\Delta M_s = 1$ transitions with an average spacing of 78 G. This is essentially half of the value from the doped-sample spectrum, as it should be.[34]

Computer simulations were performed using the two sets of copper monomer g values given above. The relative orientation of the **g** tensor and the intercopper vector is important. A number of reasonable η and ξ angles, where η and ξ relate the principal g axes to those of the zero-field **D** tensor (principal axis of which is assumed to lie along the Cu–Cu vector **r**), were tried.

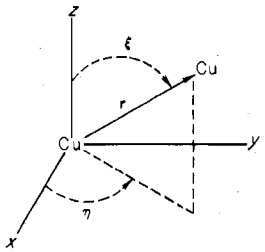

The dimer $[Cu_2(Me_5dien)_2(N_3)_2]^{2+}$ has a Cu–Cu distance of 5.2276 Å, and when this value was used in the computer program to determine the magnitude of the dipolar zero-field splitting for each signal, no features below ca. 2580 G were predicted. This was found to be the case for any setting of η and ξ angles and also for either set of monomer-like g values. On the contrary, the observed EPR spectrum (Figure 9) for $[Cu_2(Me_5dien)_2(N_3)_2](BPh_4)_2$ shows zero-field split features at 2125 and 2410 G. An estimate of the maximum dipole–dipole zero-field splitting possible when Cu–Cu = 5.2276 Å can be calculated from eq 1.[35] In this equation, θ is the angle

$$|D_{dd}| = \frac{0.325g^2}{R^3}\langle 1 - 3\cos^2\theta\rangle \qquad (1)$$

between the principal axis of the **D** tensor and the applied magnetic field, D_{dd} is given in cm^{-1}, and the Cu–Cu distance R is in Å. The maximum value of D_{dd} is obtained when θ = 0°. If g is taken as 2.220 (i.e., the $g_{\parallel}$ value for the SP monomer) and R as 5.2276 Å, $|D_{dd}|$ is calculated to be 0.022 cm^{-1}. This is essentially an order of magnitude less than the 0.159 cm^{-1} zero-field splitting seen for the g feature in the spectrum of $[Cu_2(Me_5dien)_2(N_3)_2](BPh_4)_2$. Thus, the interesting conclusion from the computer simulation attempts and this simple calculation is that *the observed zero-field splittings for these compounds greatly exceed the expected dipole–dipole splittings and must include sizable contributions from pseudodipolar zero-field interactions.*

Pseudodipolar zero-field interactions in such copper(II) dimers result from spin–orbit admixture of various excited states into the ground state manifold (i.e., singlet and triplet states).[39] In an antiferromagnetic exchange-interacting copper(II) dimer, the lowest energy state is a singlet with a triplet state at $2J$ higher in energy ($\mathcal{H} = -2J\hat{S}_1\cdot\hat{S}_2$) and these two states can be thought of as arising from the interaction of the two doublet states of the corresponding monomeric copper(II) complexes. There can also be exchange interactions in various excited states of the copper(II) dimer. This will lead to sets of singlet–triplet states for these dimer excited states with exchange parameters for each of the excited states (J_{ex}). Thus, the pseudodipolar zero-field interaction arises from the combined effect of an isotropic magnetic exchange interaction in the excited state and spin–orbit coupling between the ground and excited states. Several excited states could contribute. The magnitude of the pseudodipolar term is of the order of $J_{ex}\lambda^2/\Delta^2$, where Δ is the energy difference between the two states and λ is the spin–orbit coupling constant. The experimental zero-field splitting arises from a combination of the dipole–dipole (D_{dd}) and pseudodipolar (D_{pseudo}) interactions

$$D_{exptl} = D_{dd} + D_{pseudo} \qquad (2)$$

From the above EPR data and calculations, it is clear that the pseudodipolar term is predominant for the $[Cu_2(\text{"dien"})_2(N_3)_2](BPh_4)_2$. This is especially true since the D_{pseudo} term is of opposite sign to the D_{dd} term. The situation where D_{pseudo} is much larger than D_{dd} has been encountered previously.[40] For example, in the case of copper acetate, the dipolar term contributes only about 17% to the zero-field splitting.[15] Generally for a copper(II) dimer, an excited-state exchange parameter on the order of 30–100 cm^{-1} is required to generate a D_{pseudo} value of ca. 0.1–0.2 cm^{-1}. This is to be compared with the ground-state exchange parameters of −5 to −8 cm^{-1} observed for the $[Cu_2(\text{"dien"})_2(N_3)_2](BPh_4)_2$ compounds. Because there is no evidence of the presence of an excited state at remarkably low energy for these azide compounds, the large pseudodipolar term probably comes from an exchange interaction in an excited state(s) that is greater than what is observed for the ground state by magnetic susceptibilities. Generally the excited-state exchange parameters are an order of magnitude *smaller* than the ground-state values[41] and the two parameters only become comparable for orbitally degenerate ground states.[39] However, in addition to the present complexes, the di-μ-chloro copper(II) dimer $(Ph_4As)_2[Cu_2Cl_6]$[40] shows (calculated absolute values) excited-state exchange parameters of 50–80 cm^{-1} as compared to the (observed) ground-state exchange parameter[42] of +23 cm^{-1} (ferromagnetic).

The presence of a relatively large excited-state exchange interaction in the $[Cu_2(\text{"dien"})_2(N_3)_2](BPh_4)_2$ is reasonable. In the ground state, the unpaired electron at each Cu(II) center resides in an orbital which is composed primarily of metal $d_{x^2-y^2}$ and d_{z^2} atomic orbitals. Thus, the unpaired electrons in the ground state are in orbitals that are involved in σ types of interactions with the azide bridges. There are dimer excited states where the two unpaired electrons are found in orbitals that consist primarily of metal d_{xz}, d_{yz}, and d_{xy} orbitals. π-type interactions with the bridging azide ions would propagate an exchange interaction for this type of excited state. The azide ions would seemingly provide viable π-type "pathways" for exchange interactions.

Single-crystal EPR work is needed to extract accurate values of the various spin Hamiltonian parameters for these complexes. Excluding the isotropic magnetic exchange term ($-2J\hat{S}_1\cdot\hat{S}_2$), the usual spin Hamiltonian equation for an S = 1 system in a low-symmetry ligand field is

$$\mathcal{H} = \beta\hat{S}\cdot\hat{g}\cdot\hat{H} + D(\hat{S}_z^2 - {}^1/_3S^2 - {}^1/_3) + E(\hat{S}_x^2 - \hat{S}_y^2) \qquad (3)$$

In this equation, D is the axial zero-field splitting parameter and E is the nonaxial (rhombic) zero-field splitting parameter. As we have seen for D_{exptl}, each of these parameters has contributions from dipolar and pseudodipolar interactions. For randomly oriented triplet molecules, Wasserman et al.[33] used the above Hamiltonian equation and derived a set of equations for the resonance fields of six $\Delta M_s = 1$ transitions. These equations are

$$H_{x_1} = \frac{2.0023}{g_x}[(H_o - D + E)(H_o + 2E)]^{1/2}$$

$$H_{y_1} = \frac{2.0023}{g_y}[(H_o - D - E)(H_o - 2E)]^{1/2}$$

$$H_{z_1} = \frac{2.0023}{g_z}[(H_o - D)^2 - E^2]^{1/2} \qquad (4)$$

$$H_{x_2} = \frac{2.0023}{g_x}[(H_o + D - E)(H_o - 2E)]^{1/2}$$

$$H_{y_2} = \frac{2.0023}{g_y}[(H_o + D + E)(H_o + 2E)]^{1/2}$$

$$H_{z_2} = \frac{2.0023}{g_z}[(H_o + D)^2 - E^2]^{1/2}$$

In these equations, H_0 stands for the magnetic field expected for a free electron (depends upon the microwave frequency used) and D and E are expressed in gauss. Since we did not develop a good computer simulation for the X-band spectra of the $[Cu_2(\text{"dien"})_2(N_3)_2](BPh_4)_2$ compounds, the equations in (4) were used in an attempt to fit the observed resonance magnetic field positions. A least-squares fitting program was written that incorporated eq 4.

The six $\Delta M_s = 1$ EPR signals were assigned as described above for $[Cu_2(Me_5dien)_2(N_3)_2](BPh_4)_2$ and the magnetic field positions of the six resonances were least-squares fit to eq 4. This gave zero-field splitting parameters of $D = 931$ G (0.0870 cm^{-1}) and $E = 173$ G (0.0162 cm^{-1}). As can be seen in Table XIV, the agreement between observed and calculated resonance fields for the six $\Delta M_s = 1$ transitions is excellent for this compound. The fitting also gives g values which are found to be $g_x = 2.073$, $g_y = 2.084$, and $g_z = 2.191$ for this compound. If the above D, E, and g values are used, resonance fields can be calculated for the Q-band spectrum for this same compound. The H_z resonances are calculated to lie at 10 552 and 12 254 G. The smaller value does correspond with the lowest field feature in the spectrum; see Figure 8. The H_x and H_y resonances are calculated to run from 11 290 to 12 685 G, the higher of which does correspond with the highest field spectral feature. It is unfortunate that the Q-band spectrum is so broad and apparently only shows an envelope of these resonances.

Least-squares fitting the observed spectral features for $[Cu_2(Et_5dien)_2(N_3)_2](BPh_4)_2$ and $[Cu_2(dpt)_2(N_3)_2](BPh_4)_2$ gives very similar zero-field splitting parameters. The former compound has $D = 521$ G (0.0487 cm^{-1}) and $E = 62$ G (0.058 cm^{-1}) which are quite close to the values for the latter compound as listed in Table XIV. The dpt compound has $g_x = 2.090$, $g_y = 2.081$, and $g_z = 2.216$ as expected for a SP copper(II) environment. On the other hand, the Et_5dien compound gives the curious values of $g_x = 2.133$, $g_y = 2.076$, and $g_z = 2.206$. Perhaps some other assignment would be possible for the Et_5dien compound. As with the Me_5dien compound, the Q-band spectra for these two compounds are also relatively broad making it difficult to assign individual features with any certainty.

The temperature dependencies seen for the X-band EPR spectra of the Me_5dien (Figure 9), Et_5dien (Figure 10), and dpt (Figure 11) compounds are interesting. As can be seen in Figure 3, it is likely that the dimers in these undoped solids are reasonably well isolated. The observed line widths consist of contributions from exchange, dipolar, pseudodipolar, and hyperfine interactions. The different dependencies that are seen for the three compounds do *not* seem to simply reflect a variation in any one of these interactions; however, it is interesting that the compound Me_5dien which clearly exhibits the largest zero-field splittings is also the one that shows the most dramatic temperature dependence.

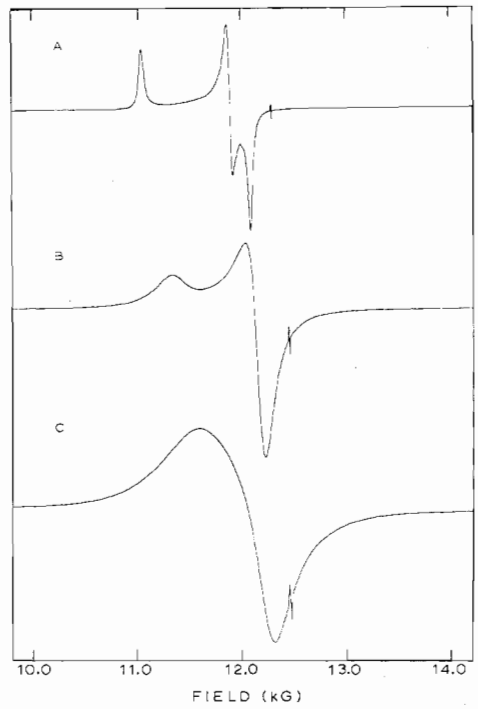

Figure 12. Q-Band (~35 GHz) EPR spectra of powdered samples of $[Cu_2(dpt)_2(N_3)_2](ClO_4)_2$ (A), $[Cu_2(Me_5dien)_2(N_3)_2](ClO_4)_2$ (B), and $[Cu_2(Et_5dien)_2(N_3)_2](ClO_4)_2$ (C) recorded at ~110 K with DPPH for frequency calibration.

In order to investigate the counterion dependence of the exchange and zero-field interactions, the perchlorate salts of the same di-μ(1,3)-azido copper(II) dimers were prepared. The Q-band EPR spectra for the ClO_4^- salts are presented in Figure 12 and can be seen to have much narrower line widths than were observed for the analogous BPh_4^- compounds as shown in Figure 8. Tracing A of Figure 12 illustrates the Q-band spectrum of $[Cu_2(dpt)_2(N_3)_2](ClO_4)_2$ which consists of signals at g values of 2.228, 2.069, and 2.038. This pattern of g values is suggestive of a SP copper(II) ion coordination geometry and is similar to that deduced for the dpt–BPh_4^- compound in Table XIV. The splitting in the "perpendicular" region is not found in the X-band spectrum of this ClO_4^- compound which suggests its origin as g-value anisotropy rather than zero-field splitting. The line widths in the X-band spectrum remain essentially unchanged from 300 to 6 K with only a parallel and perpendicular signal observable. Also, no $\Delta M_s = 2$ signal could be located around 1500 G. A crystal structure is needed to understand why this compound does not show any indications of an exchange interaction in its susceptibility data.

Tracing B of Figure 12 displays the Q-band EPR spectrum for $[Cu_2(Me_5dien)_2(N_3)_2](ClO_4)_2$ taken at ca. 110 K. Only a slight narrowing of the spectral features is seen in cooling the sample from ca. 300 to 100 K. The g values of 2.200 and 2.059 appear reasonable for a compound with SP copper(II) ion coordination geometries. The Q-band signals for this compound are somewhat broader than they are for the dpt–ClO_4^- compound. The X-band EPR spectrum clearly shows the effect of this broadening. At 300 K, a single isotropic signal is observed at $g = 2.107$. Upon cooling the sample to 80 K, the half-width at half-height maximum (hwhm) decreases from ca. 440 G at 300 K to ca. 200 G and remains relatively constant down to 6 K. It is interesting that no $\Delta M_s = 2$ signal could be found around 1500 G for this compound. The dimeric nature of the compound is substantiated, however, by the magnetic susceptibility data which gave $J = -3.1$ cm^{-1}.

Table XIV. Least-Squares Fitting Parameters for the ~6 K EPR Spectra of Azide-Bridged Copper(II) Dimers

Compd	g_x	g_y	g_z	D, G (cm^{-1})	E, G (cm^{-1})	X-band fields,[a] G Obsd	Calcd
$[Cu_2(Me_5dien)_2(N_3)_2](BPh_4)_2$[b]	2.073	2.084	2.191	931 (0.0870)	173 (0.0162)	2903	2903
						2410	2411
						2125	2124
						3307	3307
						3815	3815
						3828	3828
$[Cu_2(Et_5dien)_2(N_3)_2](BPh_4)_2$[c]	2.133	2.076	2.206	521 (0.0487)	62 (0.0058)	2920	2892
						2827	2798
						2455	2487
						3183	3208
						3457	3480
						3456	3432
$[Cu_2(dpt)_2(N_3)_2](BPh_4)_2$[d]	2.090	2.081	2.216	525 (0.0491)	83 (0.0078)	3035	2981
						2817	2759
						2410	2474
						3197	3246
						3461	3506
						3470	3423
$[Cu_2(Et_5dien)_2(N_3)_2](ClO_4)_2$[e]	2.098	2.078	2.051	660 (0.0617)	62 (0.0058)	3028	2867
						2890	2721
						2360	2541
						3183	3321
						3410	3540
						3950	3830

[a] The observed resonance fields are least-squares fit to eq 4 to give the calculated resonance fields. The resonance fields are given in the order H_{x_1}, H_{y_1}, H_{z_1}, H_{x_2}, H_{y_2}, and H_{z_2}. [b] Q-Band resonance fields (G) were calculated to be H_{x_1} = 11 842, H_{y_1} = 11 290, H_{z_1} = 10 552, H_{x_2} = 12 240, H_{y_2} = 12 685, and H_{z_2} = 12 254. [c] Q-Band resonance fields (G) were calculated to be H_{x_1} = 11 555, H_{y_1} = 11 697, H_{z_1} = 10 854, H_{x_2} = 11 870, H_{y_2} = 12 378 and H_{z_2} = 11 798. [d] Q-Band resonance fields (G) were calculated to be H_{x_1} = 11 823, H_{y_1} = 11 632, H_{z_1} = 10 805, H_{x_2} = 12 086, H_{y_2} = 12 378, and H_{z_2} = 11 754. [e] Q-Band resonance fields (G) were calculated to be H_{x_1} = 11 679, H_{y_1} = 11 614, H_{z_1} = 11 542, H_{x_2} = 12 130, H_{y_2} = 12 430, and H_{z_2} = 12 830.

It is interesting that both the dpt and Me_5dien perchlorate compounds do not show zero-field splittings in their EPR spectra. Perhaps very weak *interdimer* magnetic exchange interactions propagated by the ClO_4^- anions are present.

The greatest exchange interaction in this series of di-μ-(1,3)-azido copper(II) dimers was found in $[Cu_2(Et_5dien)_2(N_3)_2](ClO_4)_2$. The Q-band EPR spectrum of this compound at ca. 110 K is given in Figure 12, tracing C. A single asymmetric derivative is found at g = 2.074 which remains essentially unchanged from 300 to 100 K. The temperature dependence of the X-band EPR spectrum is shown in Figure 13. At 300 K, there is a single isotropic signal (g = 2.099) with a hwhm of 520 G. The signal even tails into the ΔM_s = 2 region, perhaps obscuring this signal. Cooling the sample to 80 K results in a sharpening of the signal (g = 2.116) to a hwhm of 300 G and this allows the detection of a ΔM_s = 2 signal of about 0.01 times the intensity of the ΔM_s = 1 signal. Further sharpening of spectral features occurs upon decreasing the sample temperature below 80 K, and at ca. 6 K, the spectrum appears as a rhombic triplet-state spectrum where the central derivative (g = 2.111) has a hwhm of about 100–140 G. Two shoulders appear on this derivative at 2890 and 3410 G. Further downfield and upfield are another pair of zero-field split lines at 2360 and 3950 G. Various assignments were tried for these five features. The assignment which fits best to eq 4 is given in Table XIV. Least-squares fitting of these signals to the equations gives D = 660 G (0.0617 cm^{-1}) and E = 62 G (0.0058 cm^{-1}). As can be seen in Table XIV, the fit of the $[Cu_2(Et_5dien)_2(N_3)_2](ClO_4)_2$ spectrum is the poorest fit for all four compounds. At ca. 6 K, the X-band spectrum does show a ΔM_s = 2 signal which has gained intensity relative to the ΔM_s = 1 signal (now it is ca. 0.05 times the intensity). No hyperfine structure can be resolved on the ΔM_s = 2 signal. It is interesting that only this Et_5dien–ClO_4^- compound shows some resolution and consequently zero-field splittings at low temperature. Perhaps the *inter*dimer exchange interaction is essentially absent in this one perchlorate because the Et_5dien ligand provides sufficient insulation for the copper(II) ions.

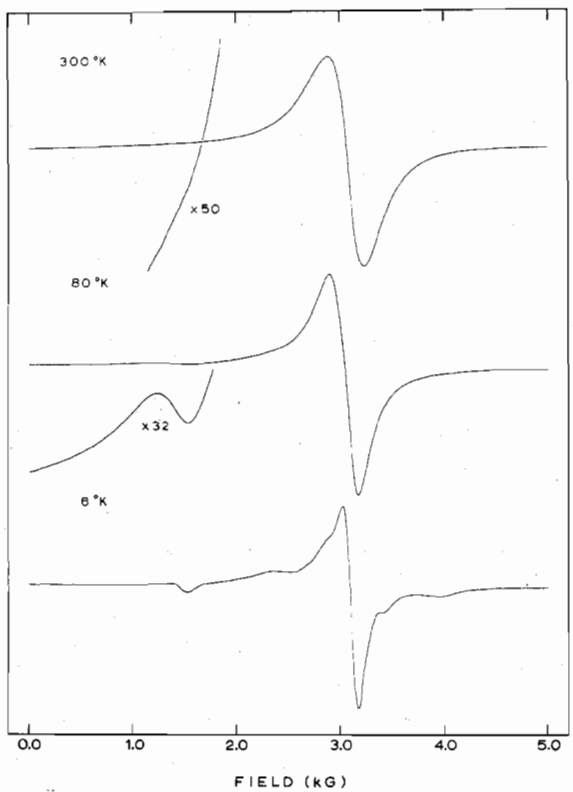

Figure 13. X-Band EPR spectra of all visible features of a powdered sample of $[Cu_2(Et_5dien)_2(N_3)_2](ClO_4)_2$ recorded at various temperatures with frequencies of 9.0868 GHz (300 K), 9.0890 GHz (80 K), and 9.1441 GHz (6 K).

Conclusions

The x-ray structure of $[Cu_2(Me_5dien)_2(N_3)_2](BPh_4)_2$ revealed the first instance of a di-μ(1,3)-azido copper(II) dimer in which the two azide ions are bridging in an end-to-end fashion. Antiferromagnetic exchange interactions are propagated by the bridging azide ions in $[Cu_2(\text{"dien"})_2(N_3)_2]X_2$, where "dien" is variously Me_5dien, Et_5dien, or dpt and X^- is BPh_4^- or ClO_4^-. The BPh_4^- counterion provides a substantial degree of magnetic dilution and the three BPh_4^- compounds show low-temperature X-band EPR spectra with resolvable copper hyperfine and zero-field splittings for *undoped* samples. Calculations show that pseudodipolar interactions dominate the observed EPR spectra and suggest that large (−50 to −100 cm^{-1}) excited-state exchange interactions are present in these di-μ(1,3)-azido dimers. This is unusual since the exchange interaction is weak (−3 to −11 cm^{-1}) for the ground state. The three ClO_4^- compounds give EPR spectra showing no resolvable copper hyperfine or zero-field splittings; the only exception is the Et_5dien compound. *Inter*dimer exchange interactions (probably very weak) are probably present in the ClO_4^- compounds.

Acknowledgment. We thank Dr. E. J. Laskowski for assistance with some of the crystallographic aspects of this work. Muin S. Haddad is to be thanked for the use of his computer program for eq 4. We are very grateful for funding of this research by National Institutes of Health Grant HL 13652 and for computing funds from the University of Illinois Research Board.

Registry No. $[Cu_2(dpt)_2(N_3)_2](ClO_4)_2$, 64682-80-0; $[Cu_2(dpt)_2(N_3)_2](PBh_4)_2$, 64682-81-1; $[Cu_2(Me_5dien)_2(N_3)_2](ClO_4)_2$, 64682-82-2; $[Cu_2(Me_5dien)_2(N_3)_2](BPh_4)_2$, 61651-90-9; $[Cu_2(Et_5dien)_2(N_3)_2](ClO_4)_2$, 64682-49-1; $[Cu_2(Et_5dien)_2(N_3)_2](BPh_4)_2$, 64682-50-4; $Cu(Et_5dien)(N_3)_2$, 64682-51-5; $Cu(Me_5dien)(N_3)_2$, 64682-52-6; $[Zn_2(Me_5dien)_2(N_3)_2](BPh_4)_2$, 64682-54-8.

Supplementary Material Available: Tables I (analytical data), IV (anisotropic thermal parameters for $[Cu_2(Me_5dien)_2(N_3)_2](BPh_4)_2$), VI (least-squares planes for the same compound), VII–XII (experimental and calculated magnetic susceptibility data for six di-μ(1,3)-azido complexes with Me_5dien, Et_5dien, or dpt ligands and BPh_4^- or ClO_4^- counterions), and final values of $|F_o|$ and $|F_c|$ for $[Cu_2(Me_5dien)_2(N_3)_2](BPh_4)_2$ (34 pages). Ordering information is given on any current masthead page.

References and Notes

(1) Part 11 of this series: C. G. Pierpont, L. C. Francesconi, and D. N. Hendrickson, *Inorg. Chem.*, **16**, 2367 (1977).
(2) Camille and Henry Dreyfus Teacher-Scholar Fellow, 1972–1977; A. P. Sloan Foundation Fellow, 1976–1978.
(3) T. R. Felthouse, E. J. Laskowski, and D. N. Hendrickson, *Inorg. Chem.*, **16**, 1077 (1977).
(4) W. Beck and W. P. Fehlhammer, *MTP Int. Rev. Sci.: Inorg. Chem., Ser. One*, **2**, 253 (1972).
(5) U. Müller, *Struct. Bonding (Berlin)* **14**, 141 (1973).
(6) Z. Dori and R. F. Ziolo, *Chem. Rev.*, **73**, 247 (1973).
(7) G. W. Bushnell and M. A. Khan, *Can. J. Chem.*, **52**, 3125 (1974).
(8) R. F. Ziolo, A. P. Gaughan, Z. Dori, C. G. Pierpont, and R. Eisenberg, *Inorg. Chem.*, **10**, 1289 (1971).
(9) (a) I. Agrell, *Acta Chem. Scand.*, **21**, 2647 (1967); (b) R. Söderquist, *Acta Crystallogr., Sect. B*, **24**, 450 (1968); (c) I. Agrell and S. Lamnevik, *Acta Chem. Scand.*, **22**, 2038 (1968).
(10) D. M. Duggan and D. N. Hendrickson, *Inorg. Chem.*, **12**, 2422 (1973).
(11) G. R. Hall, D. M. Duggan, and D. N. Hendrickson, *Inorg. Chem.*, **14**, 1956 (1975).
(12) T. R. Felthouse, E. J. Laskowski, D. S. Bieksza, and D. N. Hendrickson, *J. Chem. Soc., Chem. Commun.*, 777 (1976).
(13) Supplementary material.
(14) R. Shelby, R. F. Ziolo, Z. Dori, and H. B. Gray, unpublished results.
(15) B. Bleaney and K. D. Bowers, *Proc. R. Soc. London, Ser. A*, **214**, 451 (1952).
(16) (a) H. P. Hansen, F. Herman, J. D. Lea, and S. Skillman, *Acta Crystallogr.*, **17**, 1040 (1964); (b) D. T. Cromer and J. B. Mann, *Acta Crystallogr., Sect. A*, **24**, 321 (1968); (c) "International Tables for X-ray Crystallography", Vol. III, Kynoch Press, Birmingham, England, 1962.
(17) F. Wagner, M. T. Mocella, M. J. D'Aniello, Jr., A. H.-J. Wang, and E. K. Barefield, *J. Am. Chem. Soc.*, **96**, 2625 (1974).
(18) C. G. Pierpont, D. N. Hendrickson, D. M. Duggan, F. Wagner, and E. K. Barefield, *Inorg. Chem.*, **14**, 604 (1975).
(19) I. Agrell, *Acta Chem. Scand.*, **20**, 1281 (1966).
(20) I. Agrell, *Acta Chem. Scand.*, **23**, 1667 (1969).
(21) R. F. Ziolo, M. Allen, D. D. Titus, H. B. Gray, and Z. Dori, *Inorg. Chem.*, **11**, 3044 (1972).
(22) B. F. Hoskins and F. D. Whillans, *Coord. Chem. Rev.*, **9**, 365 (1972–1973).
(23) The labeling scheme used for the BPh_4^- counterion is the same as we used before; see D. M. Duggan and D. N. Hendrickson, *Inorg. Chem.*, **13**, 1911 (1974).
(24) M. DiVaira and P. L. Orioli, *Chem. Commun.*, 590 (1965).
(25) B. G. Segal and S. J. Lippard, *Inorg. Chem.*, **13**, 822 (1974).
(26) Z. Dori, R. Eisenberg, and H. B. Gray, *Inorg. Chem.*, **6**, 483 (1967).
(27) (a) D. M. Duggan and D. N. Hendrickson, *Inorg. Chem.*, **13**, 2056 (1974); (b) E. J. Laskowski, D. M. Duggan, and D. N. Hendrickson, *ibid.*, **14**, 2449 (1975).
(28) R. G. Jungst, Ph.D. Thesis, University of Illinois, 1976.
(29) R. A. Bauer, W. R. Robinson, and D. W. Margerum, *J. Chem. Soc., Chem. Commun.*, 289 (1973).
(30) K. Singh, *Trans. Faraday Soc.*, **67**, 2436 (1971).
(31) D. M. Duggan and D. N. Hendrickson, *Inorg. Chem.*, **13**, 2929 (1974).
(32) The disparity between the relative intensity differences of $\Delta M_s = 2$ transitions in X-band vs. Q-band spectra arises from the greater degree of mixing of the singlet- and triplet-state wave functions that is possible at fields of ca. 1400 G in the X-band case than for fields of ca. 6000 G in the Q-band case. The transition probability is inversely proportional to the square of the magnetic field; see J. F. Boas, R. H. Dunhill, J. R. Pilbrow, R. C. Srivastava, and T. D. Smith, *J. Chem. Soc. A*, 94 (1969).
(33) E. Wasserman, L. C. Snyder, and W. A. Yager, *J. Chem. Phys.*, **41**, 1763 (1964).
(34) C. P. Slichter, *Phys. Rev.*, **99**, 479 (1955).
(35) R. L. Belford, N. D. Chasteen, H. So, and R. E. Tapscott, *J. Am. Chem. Soc.*, **91**, 4675 (1969).
(36) N. D. Chasteen and R. L. Belford, *Inorg. Chem.*, **9**, 169, 2805 (1970).
(37) D. L. Gibbons, Ph.D. Thesis, University of Illinois, 1974.
(38) G. G. Belford, R. L. Belford, and J. F. Burkhalter, *J. Magn. Reson.*, **11**, 251 (1973).
(39) J. Owen and E. A. Harris in "Electron Paramagnetic Resonance", S. Geschwind, Ed., Plenum Press, New York, N.Y., 1972, pp 427–492.
(40) C. Chow and R. D. Willett, *J. Chem. Phys.*, **59**, 5903 (1973).
(41) G. F. Kokoszka, H. C. Allen, Jr., and G. Gordon, *J. Chem. Phys.*, **46**, 3013 (1967).
(42) C. Chow, R. Caputo, R. D. Willett, and B. C. Gerstein, *J. Chem. Phys.*, **61**, 271 (1974).